Electroweak penguin decays as probes of physics beyond the Standard Model

Mitesh Patel (Imperial College London)

LHC Seminar, 8th May 2012

on behalf of the LHCb Collaboration

Imperial College London

LHCb

The interest in EW penguins

- Standard Model has no tree level Flavour Changing Neutral Currents (FCNC)

- FCNC only occur as loop processes, proceed via penguin or box diagrams – sensitive to contributions from new (virtual) particles

  → Probe masses > E_{CM} of the accelerator

- e.g. $B^0 \rightarrow K^{*0}\gamma$ decay

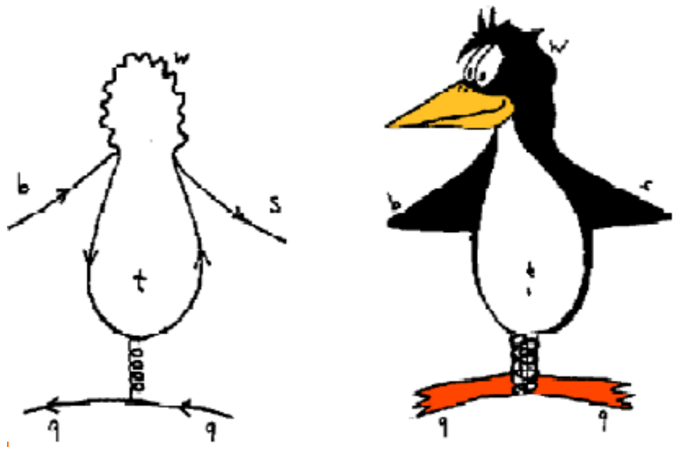

A historical example – $B^0 \to K^{*0}\gamma$

- In SM: occurs through a dominating W-t loop
- Possible NP diagrams:
- Observed by CLEO in 1993, two years before the direct observation of the top quark
  - BR was expected to be $(2\text{-}4)\times10^{-4}$
  - → measured BR = $(4.5\pm1.7)\times10^{-4}$

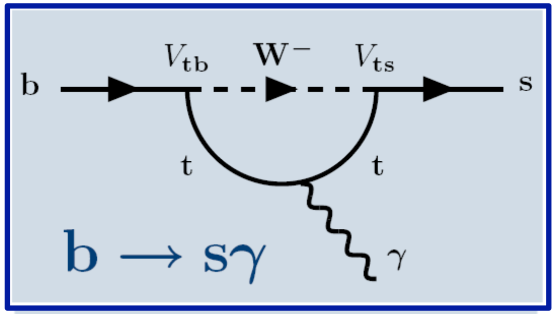

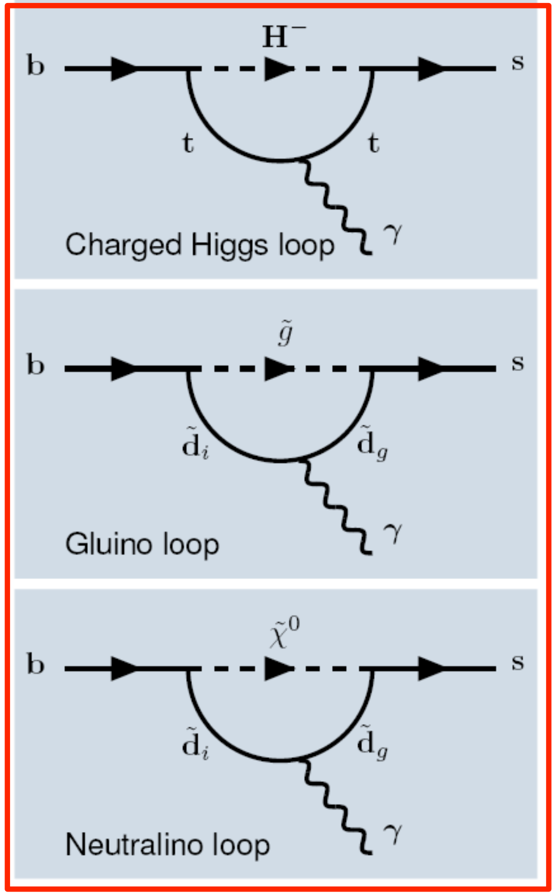

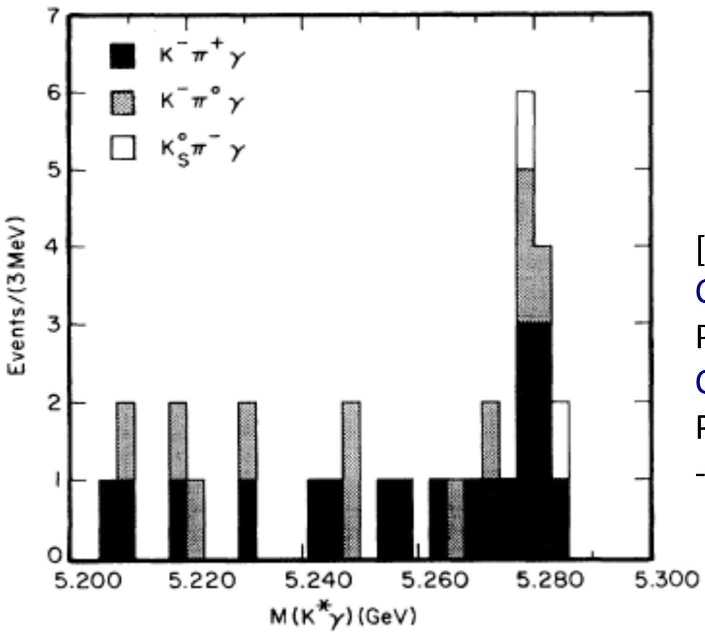

[Phys.Rev.Lett. 71 (1993) 674 - Cited by 605 records
Phys.Rev.Lett. 74 (1995) 2885 - Cited by 836 records
Phys.Rev.Lett. 87 (2001) 251807 - Cited by 565 records]

Theoretical Foundation

- The Operator Product Expansion is the theoretical tool that underpins rare decay measurements – rewrite SM Lagrangian as :

$$\mathcal{L} = \sum_i C_i O_i$$

  - "Wilson Coefficients" C_i
    - Describe the short distance part, can compute perturbatively in given theory
    - Integrate out the heavy degrees of freedom that can't resolve at some energy scale μ
  - "Operators" O_i
    - Describe the long distance, non-perturbative part involving particles below the scale μ
    - Account for effects of strong interactions and are difficult to calculate reliably

  → **Form a complete basis – can put in all operators from NP/SM**

- In *certain* observables the uncertainties on the operators cancel out – are then free from theoretical problems and measuring the Wilson Coefficients tells us about the heavy degrees of freedom – *independent of model*

Observables in EW penguin decays

- Measuring branching fraction of EW penguin decays → information on mass, coupling

- Can also make a different class of measurements – probe the helicity structure :
  - If decay mediated by Z boson – expect L&R-handed contributions, measure ratio of the two
  - If decay mediated by NP – ????

- Have two options :
  - (Only states with same polarisation/helicity can interfere) → measure time dependent CP violation where tag if have a B or a $\bar{B}$
  - Use self-tagging channels e.g. sign of $K^{\pm}$ from $K^{*0} \rightarrow K\pi$ decay indicates whether had a B or $\bar{B}$ → angular analysis

Outline

- The LHCb detector and trigger
- Angular analysis of the decay $B^0 \to K^* \mu\mu$
- The search for the decay $B^+ \to \pi^+ \mu\mu$
- The isospin asymmetry in $B \to K^* \mu\mu$ and $B \to K \mu\mu$ decays
  - Shown in public for first time … interesting results
- A_{CP} in $B^0 \to K^{*0} \gamma$

(All results from the full $1 fb^{-1}$ of integrated luminosity collected in 2011)

The Experimental Environment

- LHC produces a huge number of B decays
  - $\sigma(b\bar{b})$ = 280μb @ LHC, 7TeV (**) (approx. linear with energy)
  - $\sigma(b\bar{b})$ = 0.001μb @ B factories

- At the LHC σ(pp, inelastic) @ $\sqrt{s}$=7 TeV ~60 mb, only 1/200 events contains a b quark, looking for BR ~10^{-6}-10^{-9} - enormous demands on detector and trigger

→ The LHCb experiment

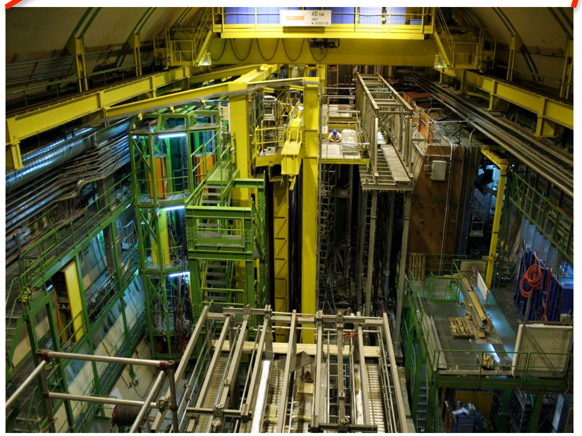

(**) LHCb, Phys. Lett. B 694 (2010) 209-216

The LHCb Experiment

- b production predominately at small polar angles
  → forward spectrometer

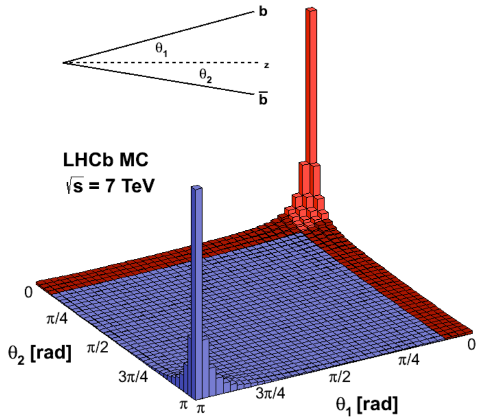

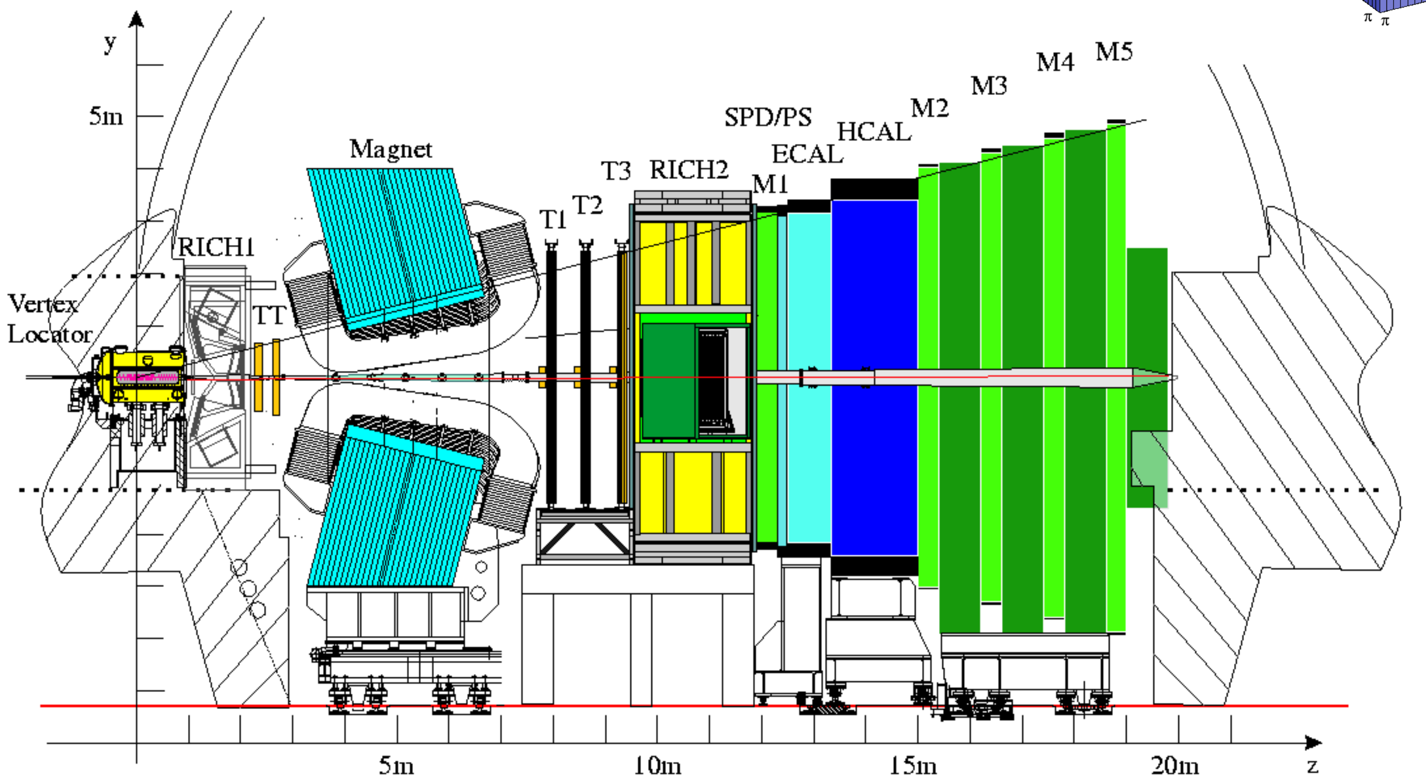

The LHCb Experiment

- B lifetime → displaced secondary vertex
  - Need few interactions/event → operate at luminosity 10–50 times lower than central detectors
  - Vertex detector capable of picking out the displaced vertex

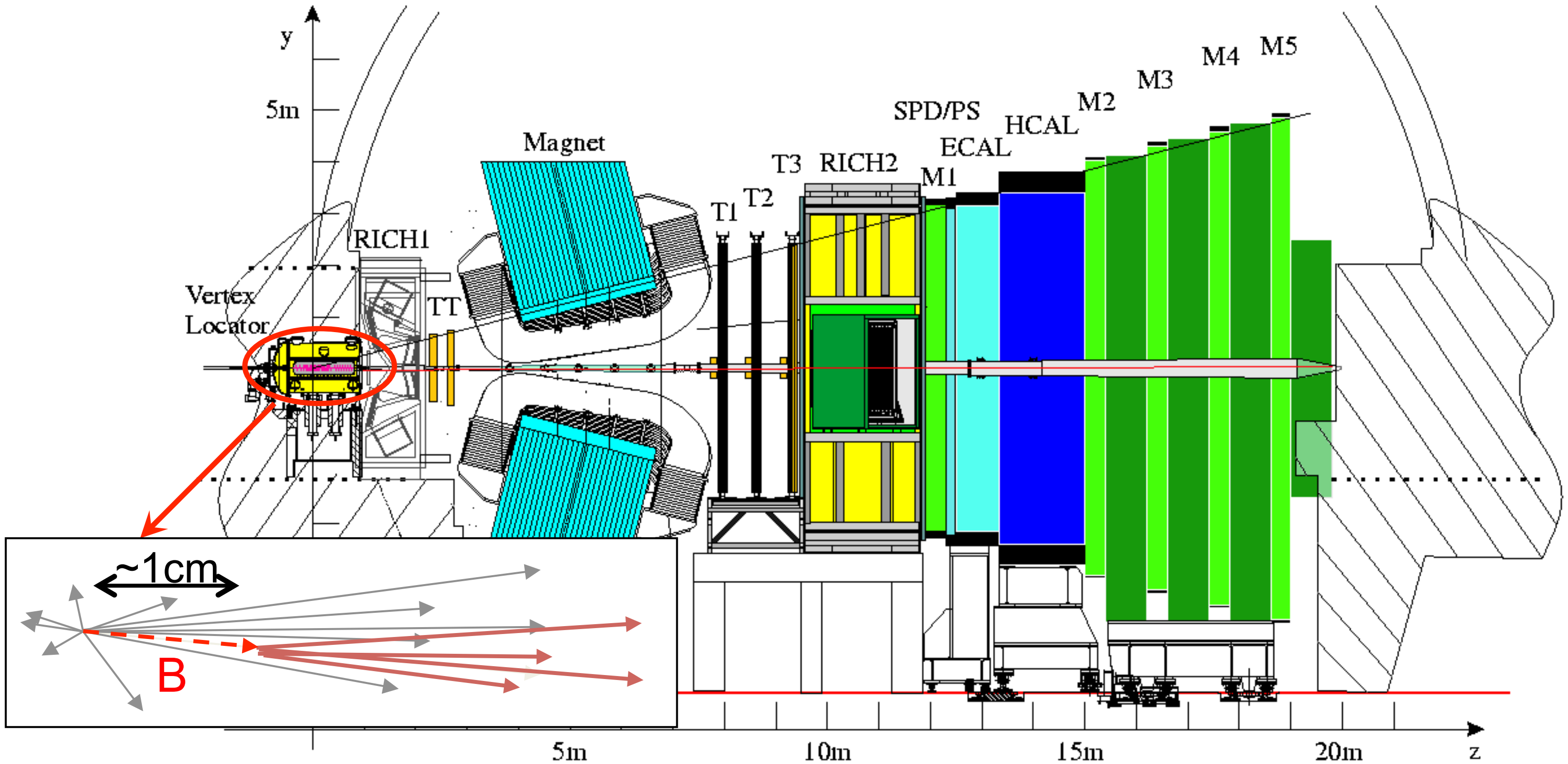

The LHCb Experiment

- B lifetime → displaced secondary vertex
  - Need few interactions/event → operate at luminosity 10–50 times lower than central detectors
  - Vertex detector capable of picking out the displaced vertex

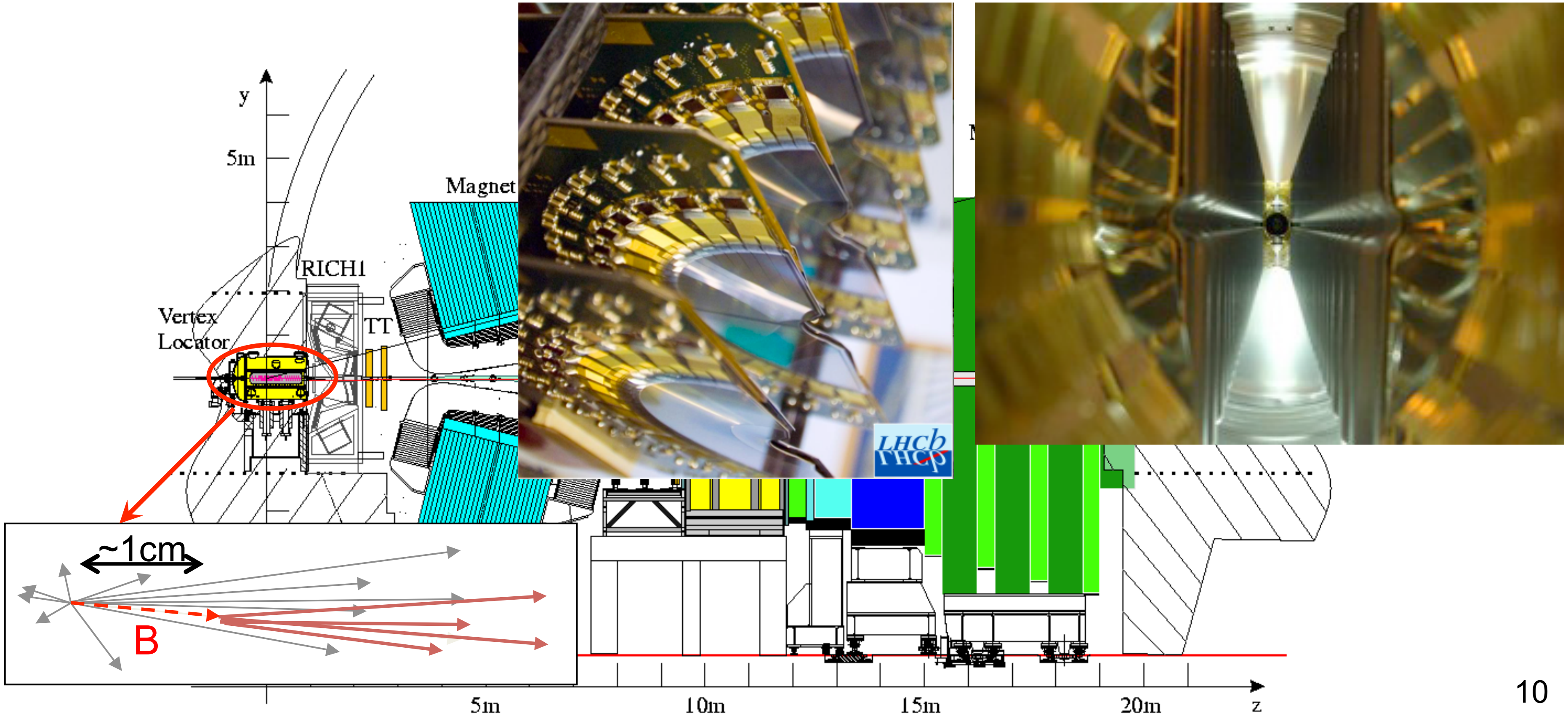

The LHCb Experiment

- Precision momentum resolution → mass resolution

	LHCb	CMS	ATLAS
Momentum Resolution	$\delta p/p$=0.4-0.6%	$\delta p_T/p_T$=1-3%	$\delta p_T/p_T$=5-6%
Mass resoln $J/\psi \rightarrow \mu\mu$	13 MeV/c^2	28 MeV/c^2 (*)	46 MeV/c^2 (**)

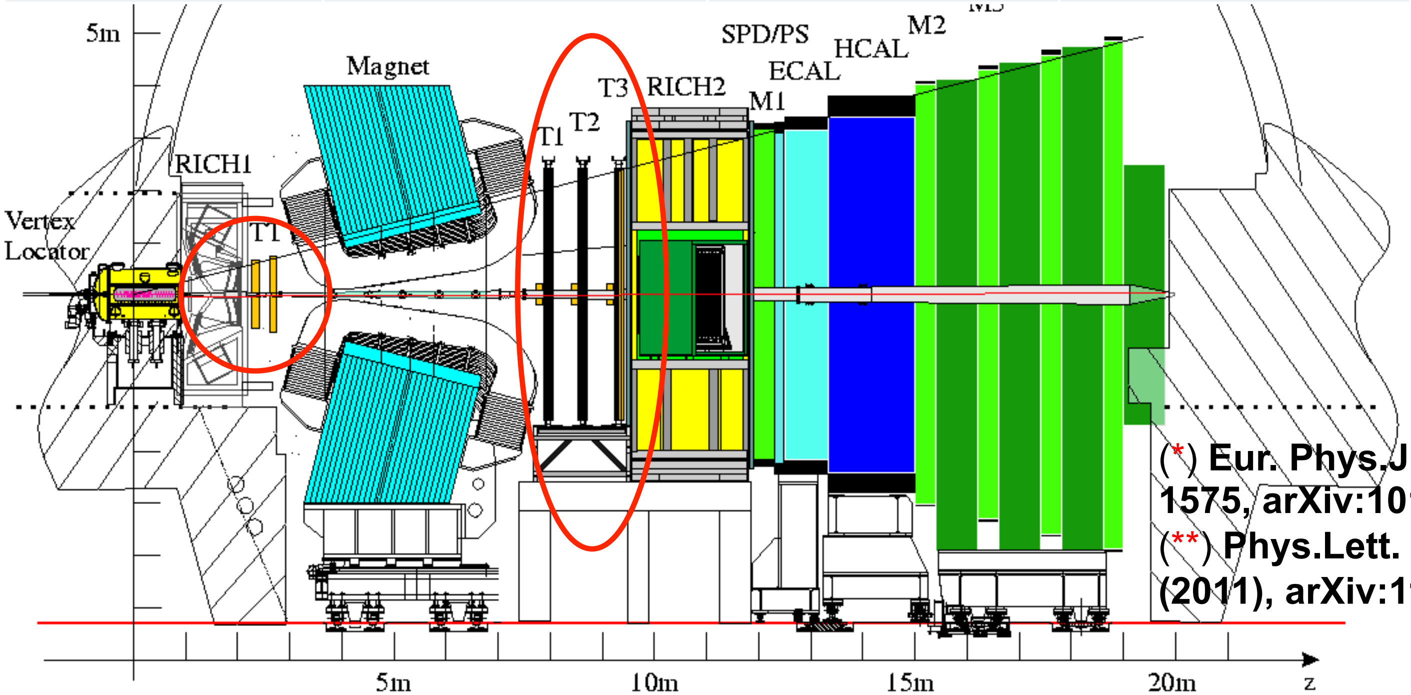

(*) Eur. Phys.J. C71 (2011) 1575, arXiv:1011.4193
(**) Phys.Lett. B697 (2011), arXiv:1104.3038v2

The LHCb Experiment

- Events dominated by pions – separating kaons (→RICH 1,2) produced in B events and muons (→M1-5) critical

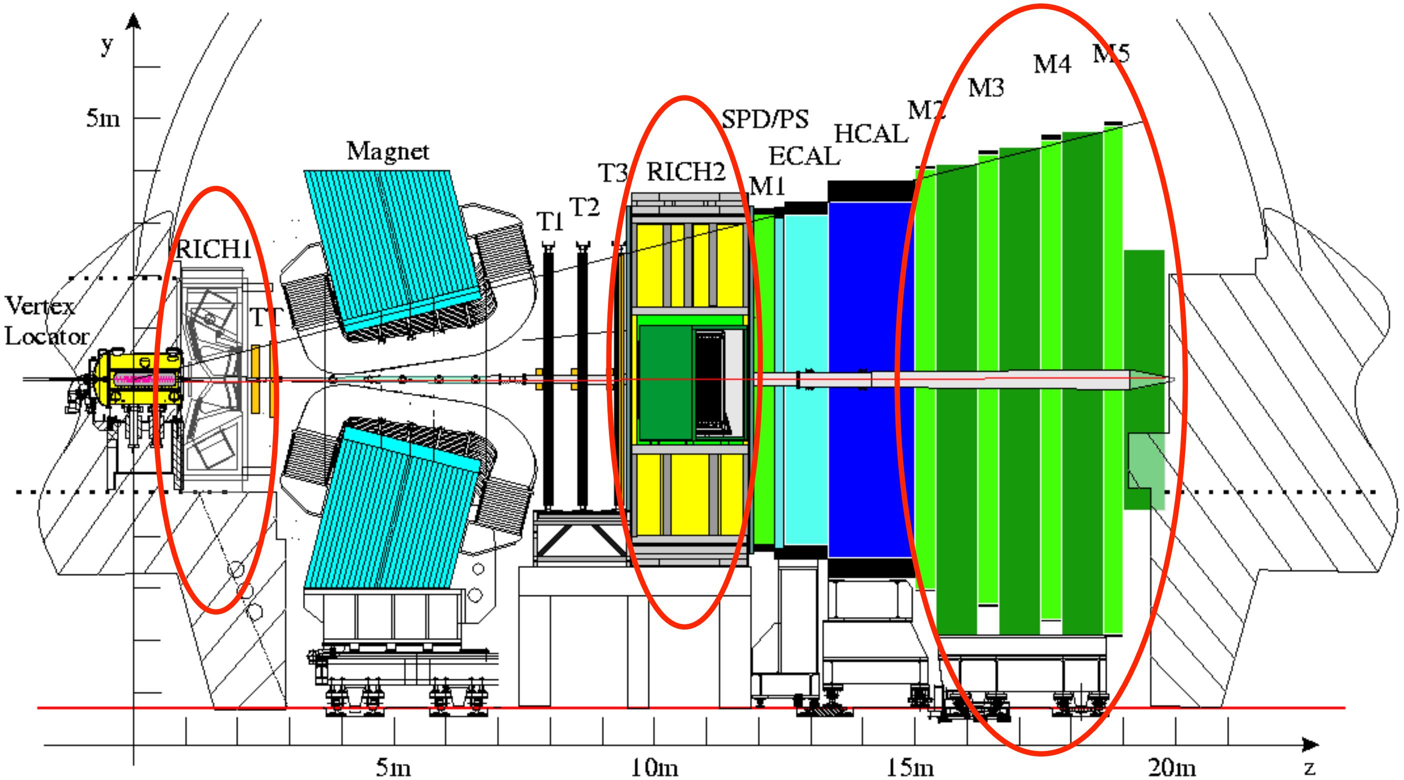

The LHCb Experiment

- Events dominated by pions – separating kaons (→RICH 1,2) produced in B events and muons (→M1-5) critical

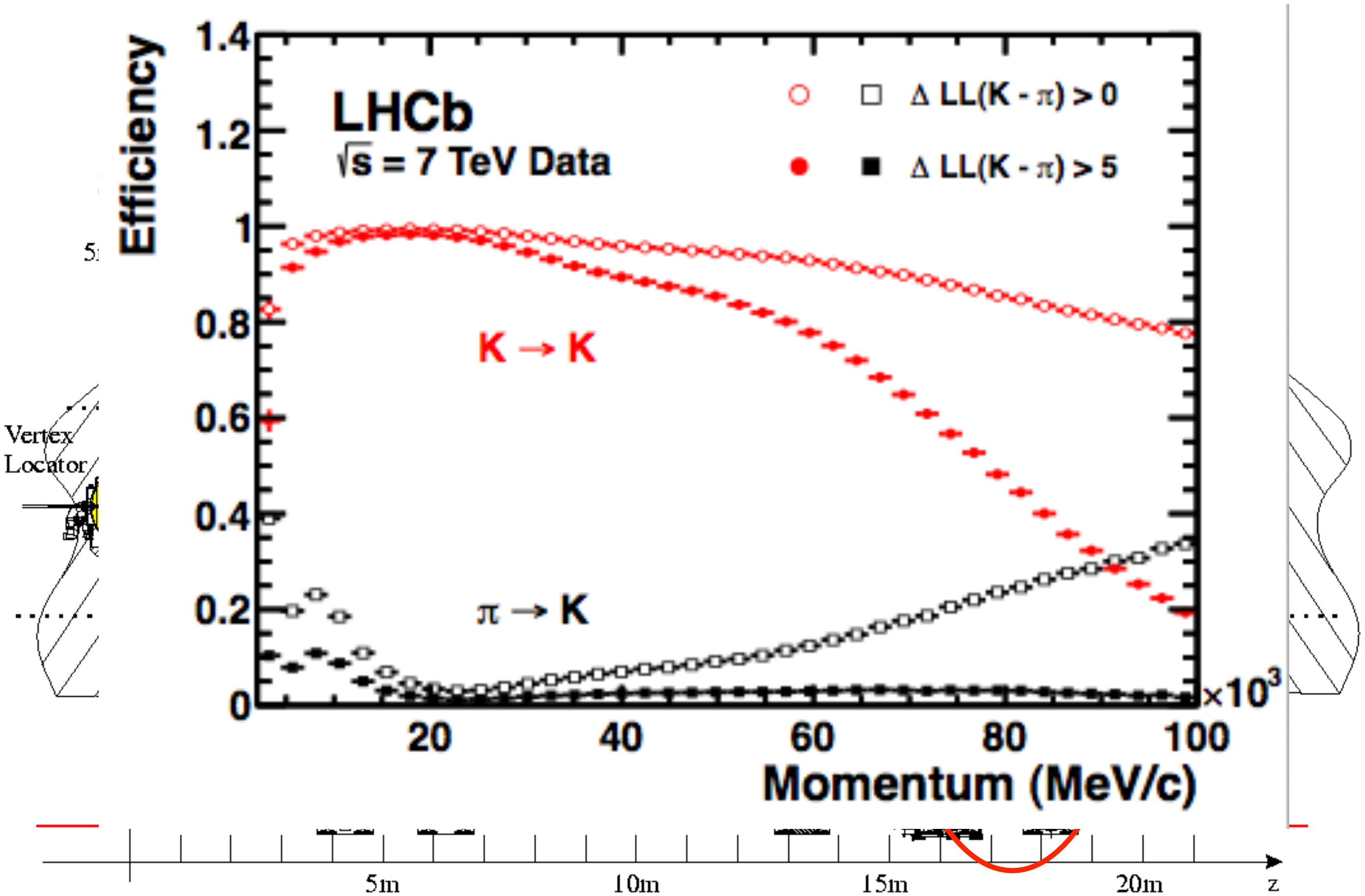

The LHCb Trigger

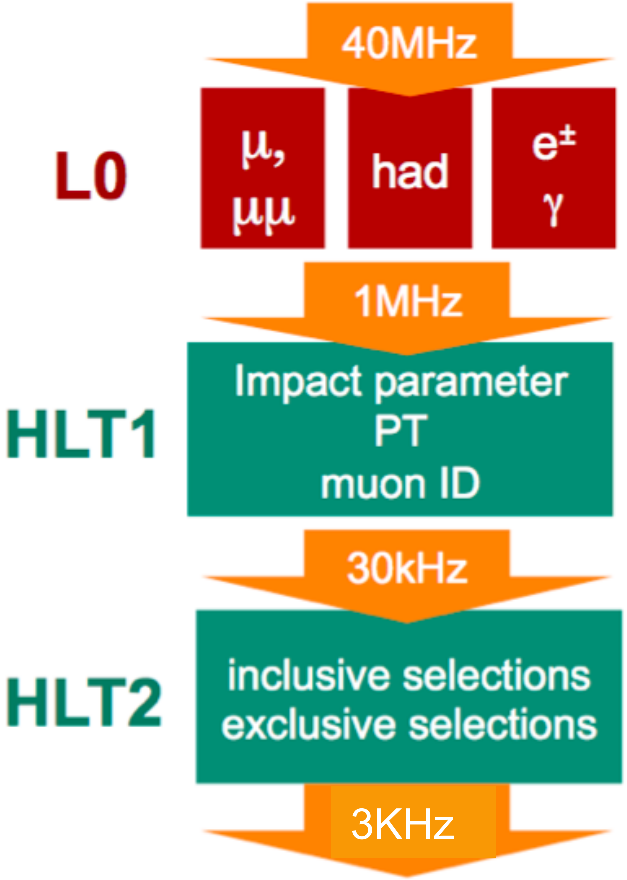

L0 Hardware	"high p_T" signals in calorimeter and muon systems
HLT1 Software	Partial reconstruction, selection based on one or two (dimuon) displaced tracks, muon ID
HLT2 Software	Global reconstruction (very close to offline) dominantly inclusive signatures – use MVA

+ Global Event Cuts for events with high multiplicity

	Charm	Had. B	Lept. B
Overall efficiency	~10%	~40%	~75-90%

- Small event size (60kB) → large bandwidth
- Allows low thresholds

$B^0 \rightarrow K^* \mu\mu$

$B^0 \to K^*\mu\mu$

- Flavour changing neutral current → loop
- Sensitive to interference between $O_{7\gamma}$, $O_{9,10}$ and their primed counterparts
- Exclusive decay → theory uncertainty from form factors
- Decay described by three angles, θ_l, θ_K and ϕ, and $q^2 = m^2_{\mu\mu}$, self-tagging → angular analysis allows to probe helicity
- Multitude of angular observables in which uncertainties cancel to some extent e.g. A_{FB} – asymmetry in θ_l distribution

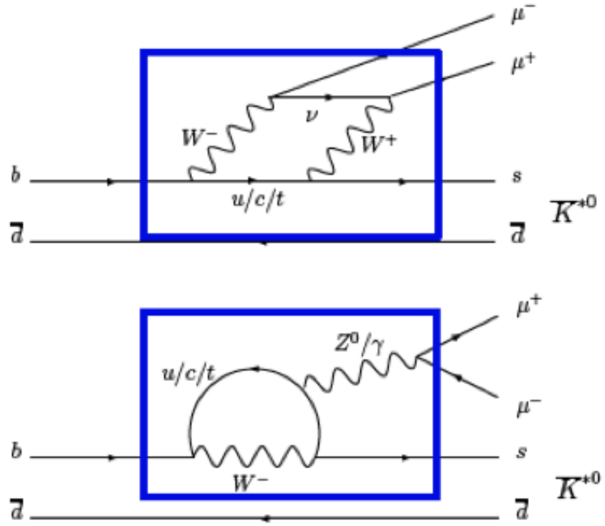

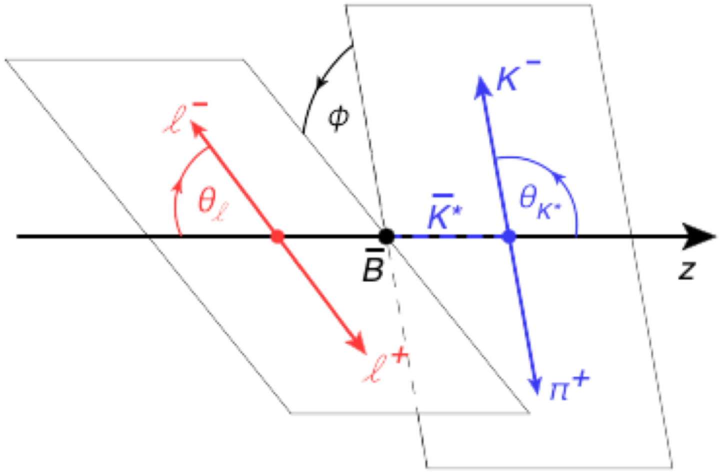

$B^0 \to K^*\mu\mu$ – angular analysis

- Full angular distribution :

$$\frac{d^4\Gamma}{d\cos\theta_\ell\, d\cos\theta_K\, d\phi\, dq^2} \propto I_1^s \sin^2\theta_K + I_1^c \cos^2\theta_K + \left(I_2^s \sin^2\theta_K + I_2^c \cos^2\theta_K\right)\cos 2\theta_\ell$$
$$+ I_3 \sin^2\theta_K \sin^2\theta_\ell \cos 2\phi + I_4 \sin 2\theta_K \sin 2\theta_\ell \cos\phi$$
$$+ I_5 \sin 2\theta_K \sin\theta_\ell \cos\phi$$
$$+ \left(I_6^s \sin^2\theta_K + I_6^c \cos^2\theta_K\right)\cos\theta_\ell + I_7 \sin 2\theta_K \sin\theta_\ell \sin\phi$$
$$+ I_8 \sin 2\theta_K \sin 2\theta_\ell \sin\phi + I_9 \sin^2\theta_K \sin^2\theta_\ell \sin 2\phi$$

- Apply "folding" technique: $\phi \to \phi+\pi$ for $\phi < 0$. This cancels terms with I_4, I_5, I_7, I_8

- Fitting these angles allows access to angular observables where the hadronic uncertainties are under control :
  - F_L, the fraction of K^{*0} longitudinal polarisation
  - A_{FB}, the forward-backward asymmetry – and zero-crossing point
  - $S_3 \propto A^2_T(1-F_L)$, the asymmetry in K^{*0} transverse polarisation
  - A_{IM}, a T-odd CP asymmetry

$B^0 \rightarrow K^*\mu\mu$ – angular analysis

- Full angular distribution :

$$
\begin{aligned}
\frac{d^4\Gamma}{d\cos\theta_\ell\, d\cos\theta_K\, d\phi\, dq^2} \quad \propto \quad & F_L \cos^2\theta_K + \frac{3}{4}(1-F_L)(1-\cos^2\theta_K) + \\
& F_L \cos^2\theta_K (2\cos^2\theta_\ell) + \\
& \frac{1}{4}(1-F_L)(1-\cos^2\theta_K)(2\cos^2\theta_\ell - 1) + \\
& S_3(1-\cos^2\theta_K)(1-\cos^2\theta_\ell)\cos 2\phi + \\
& \frac{4}{3}A_{FB}(1-\cos^2\theta_K)\cos\theta_\ell + \\
& A_{Im}(1-\cos^2\theta_K)(1-\cos^2\theta_\ell)\sin 2\phi
\end{aligned}
$$

- Apply "folding" technique: $\phi \rightarrow \phi+\pi$ for $\phi < 0$. This cancels terms with I_4, I_5, I_7, I_8

- Fitting these angles allows access to angular observables where the hadronic uncertainties are under control :
  - F_L, the fraction of K^{*0} longitudinal polarisation
  - A_{FB}, the forward-backward asymmetry – and zero-crossing point
  - $S_3 \propto A^2_T(1-F_L)$, the asymmetry in K^{*0} transverse polarisation
  - A_{IM}, a T-odd CP asymmetry

The interest in $B^0 \to K^*\mu\mu$

- Observables highly sensitive to NP contributions to $C_7^{(\prime)}$, $C_9^{(\prime)}$, $C_{10}^{(\prime)}$

W.Altmannshofer et al. [arXiv:0801.1214]

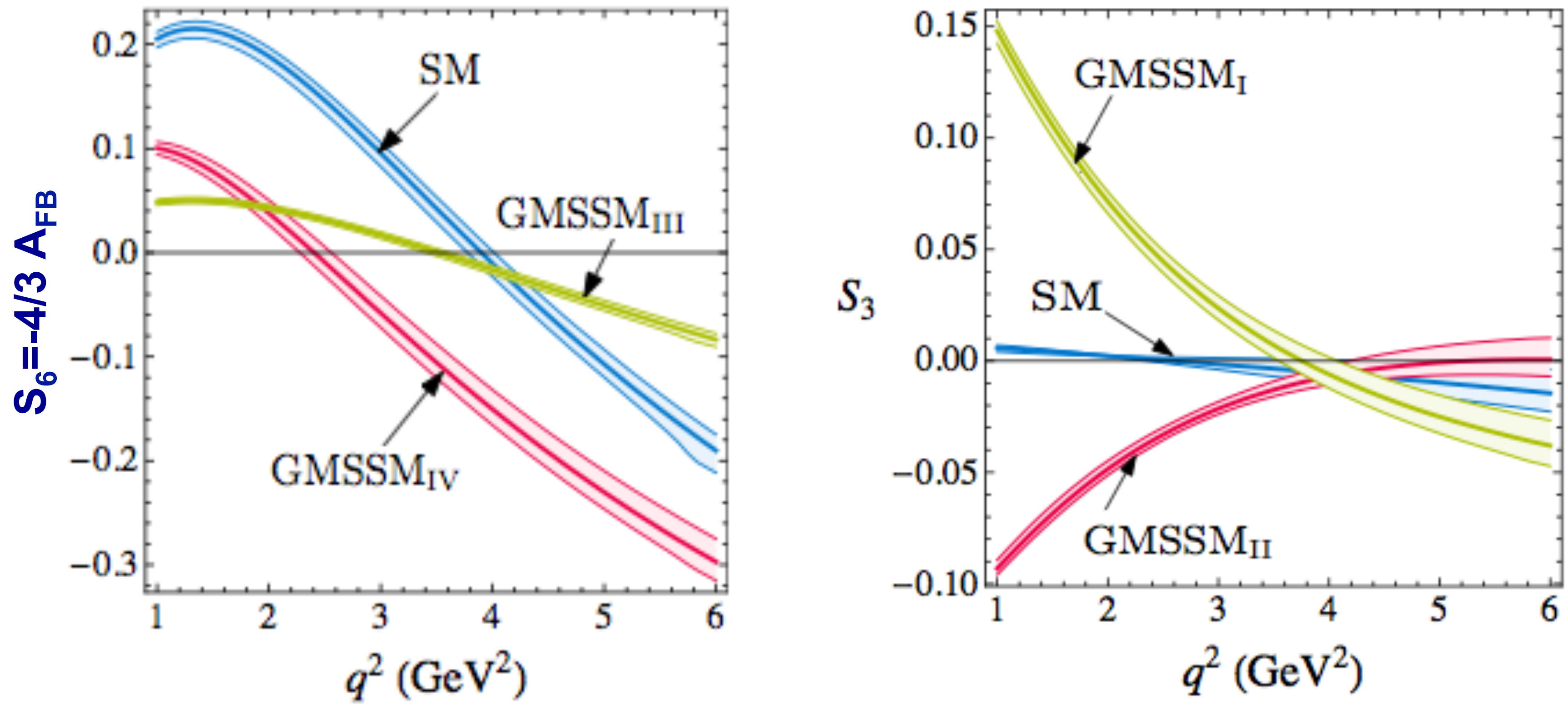

- A_{FB} zero crossing point particularly well predicted by theory

(Pre-LHC) Experimental Status

- Babar, Belle, and CDF have all measured ang. asymm. A_{FB} :

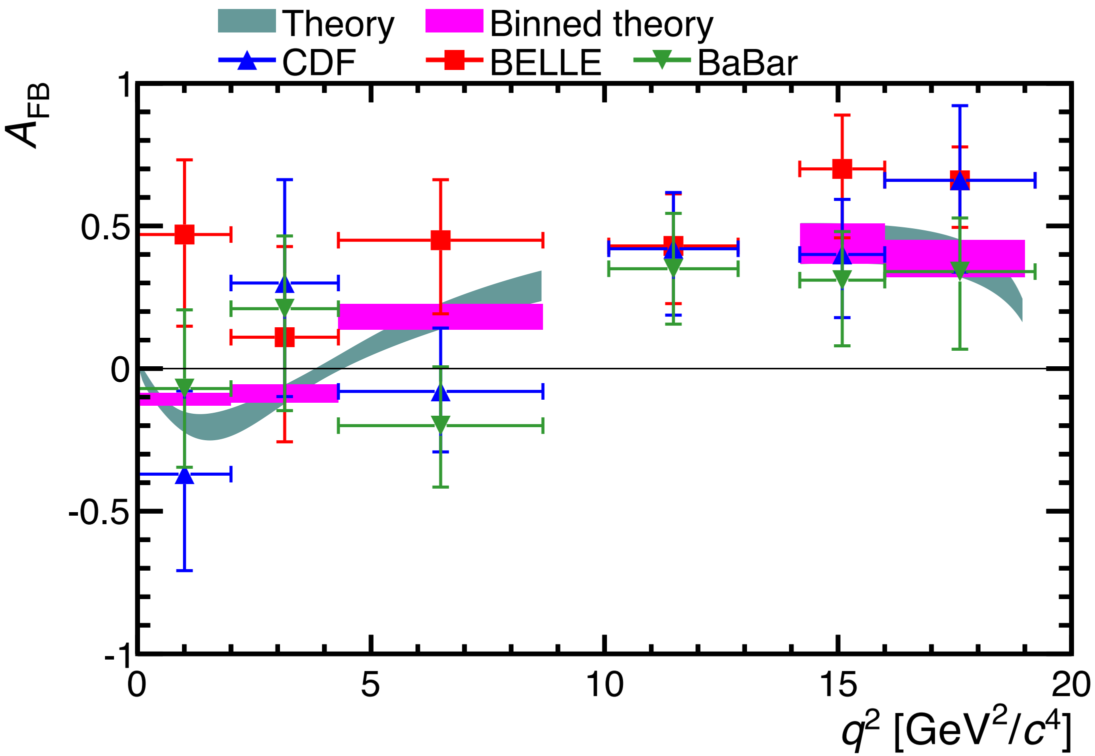

- Measurements look consistent with each other but errors still large

Theory prediction from C. Bobeth et al. [arXiv:1105.0376] (and ref. therein)

BABAR: PRL 102, 091803 (2009); CDF: arXiv:1108.0695v1; Belle: PRL 103, 171801 (2009)

LHCb Event Selection

LHCb-CONF-2012-008

- Use a Boosted Decision Tree to make event selection
  - Signal sample – $B^0 \to K^* J/\psi$ data (~100× more statistics than signal)
  - Bkgrd sample – $B^0 \to K^* \mu\mu$ mass sideband events
  - Use information about the event kinematics, vertex and track quality, impact parameter and particle identification information

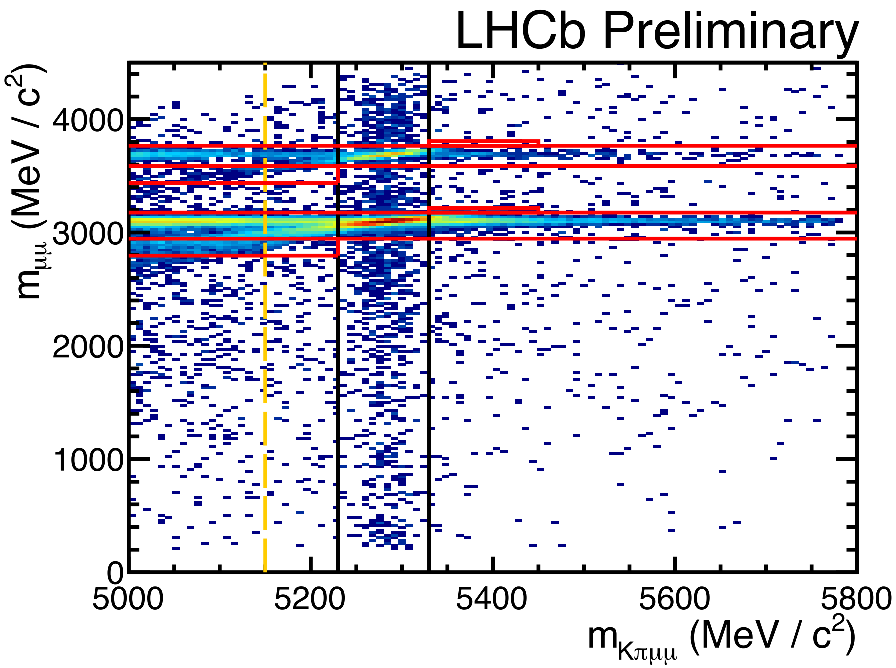

- Remove $m_{\mu\mu}$ regions containing $B^0 \to K^* J/\psi$, $B^0 \to K^* \Psi(2S)$

- Number of peaking backgrounds treated with specific vetos
  - e.g. $B^0 \to K^* J/\psi$ with $\pi \leftrightarrow \mu$ swap

→ total peaking bkgrds <2% of signal

LHCb Event Selection

- With 1.0 fb^{-1} find 900±34 signal events (BaBar + Belle + CDF ~ 600)
- B/S≈0.25 in region $5230 < m_{K\pi\mu\mu} < 5330$ MeV/c^2
- Selection does not induce further biases in angles and q^2 cf reconstruction/trigger – biases that are introduced are primarily from detector geometry – easy to model

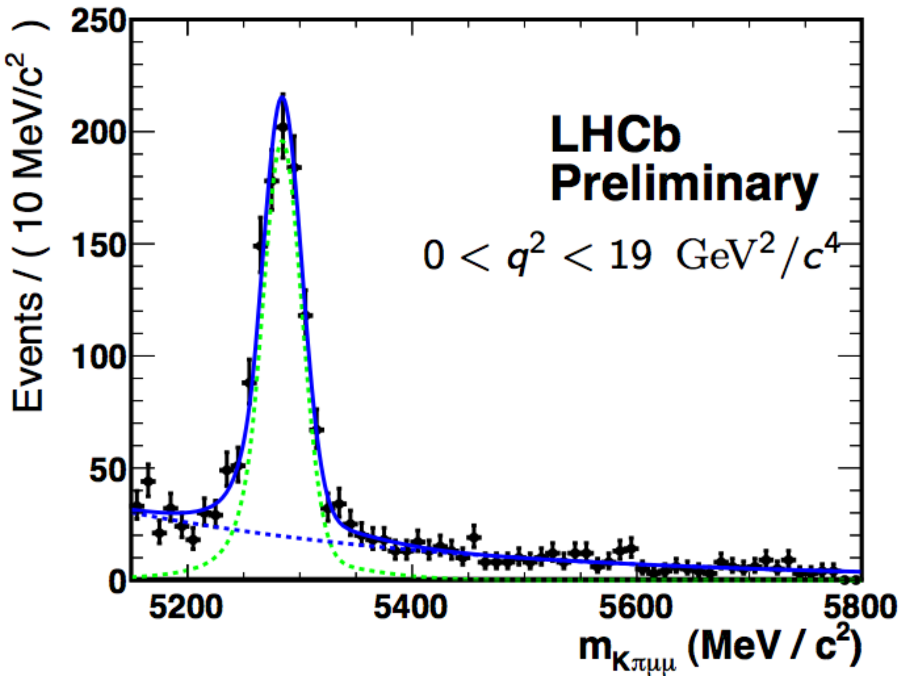

LHCb-CONF-2012-008

Acceptance Correction

- Correct angular and q^2 distributions for the effect of the detector and selection
- Use a binned acceptance correction derived from LHCb simulation
- Simulation quality verified with range of control channels which are selected from the data ($B^0 \to K^* J/\psi$, $J/\psi \to \mu\mu$, $D^* \to D^0(K\pi)\pi$)
  - Tracking efficiency
  - Hadron (mis-)identification probabilities
  - Muon (mis-)identification
  - Overall momentum and η distributions

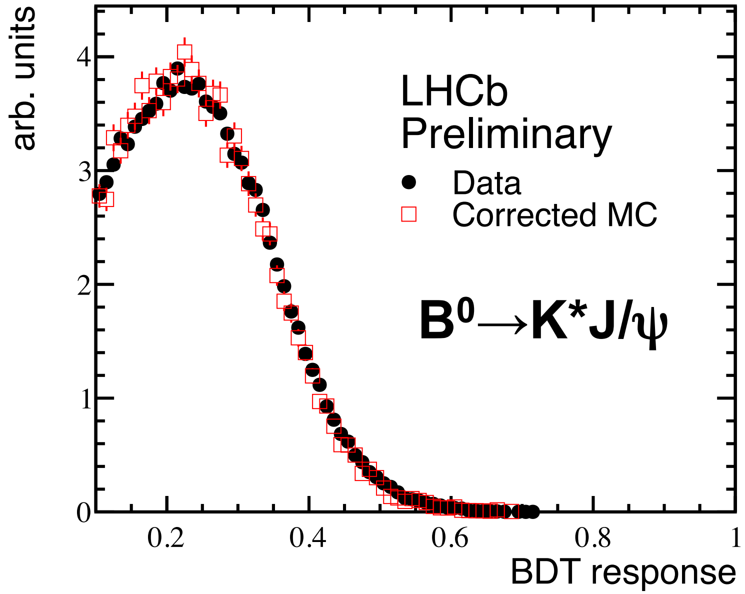

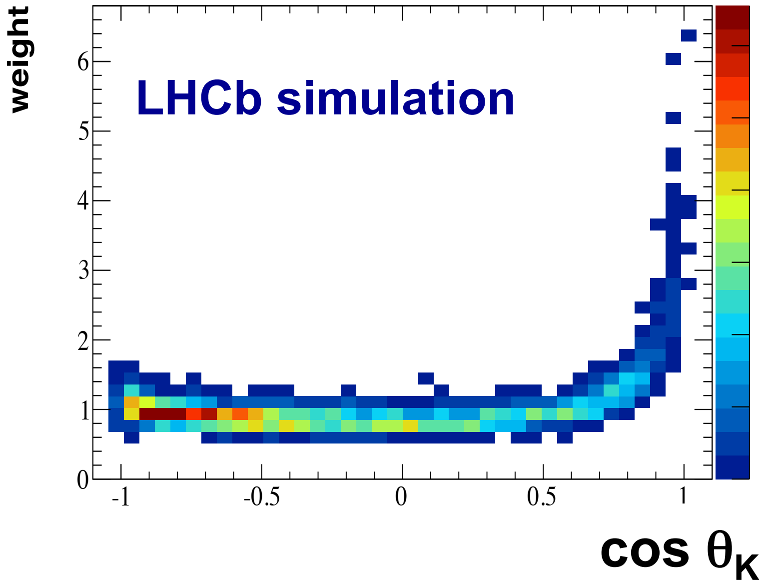

Fit Procedure and Validation

- Perform a unbinned maximum-likelihood fit to the mass and (θ_l, θ_K, ϕ) distribution in bins of q^2
- Toy simulation studies used to verify behaviour of fit
- Also validated on data using $B^0 \rightarrow K^* J/\psi$
  - A_{FB} consistent with zero, as expected
  - s-wave contribution induces an asymmetry in $\cos\theta_K$ distribution, A_{FB}^K
  - Variation of A_{FB}^K with $m_{K\pi}$ matches BaBar data(**) across $m_{K\pi}$ range

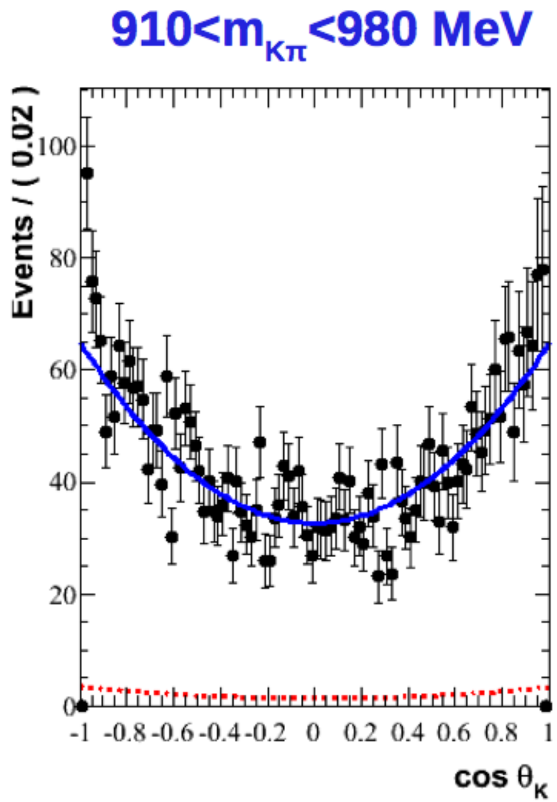

(**) BABAR: PRD 76, 031102 (2007)

Systematics

- Consider effects that are q^2-dependent or modify the angular distribution and might be incorrectly modelled by the simulation
  - Uncertainties on all of the data-driven corrections
  - Inclusion of an S-wave component
  - Knowledge of the detector acceptance
  - Variation of mass resolution with q^2
  - Uncertainty from $B(B^0 \to K^* J/\psi(\to \mu\mu))$
  - Variation of level/shape of residual peaking backgrounds
  - …

- Effects are small, measurements are statistically dominated

Event yields

LHCb-CONF-2012-008

- Observe events with >>5σ significance in each q^2 bin

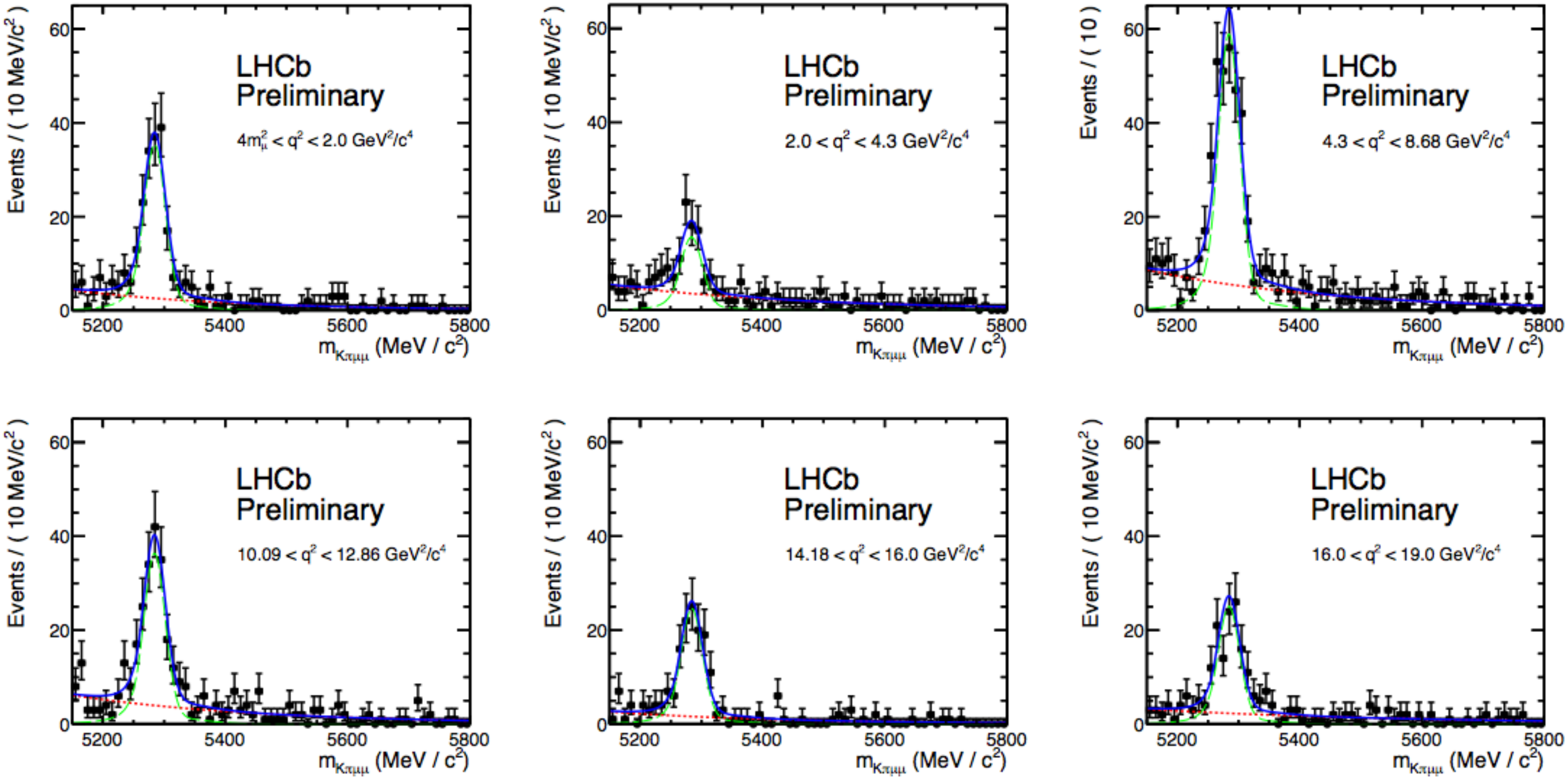

Angular Analysis Results : A_{FB}

LHCb-CONF-2012-008

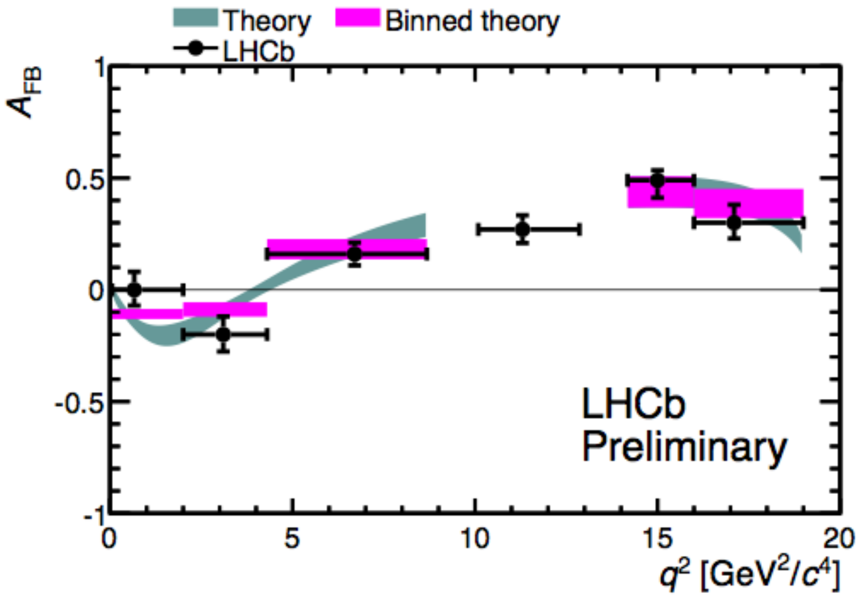

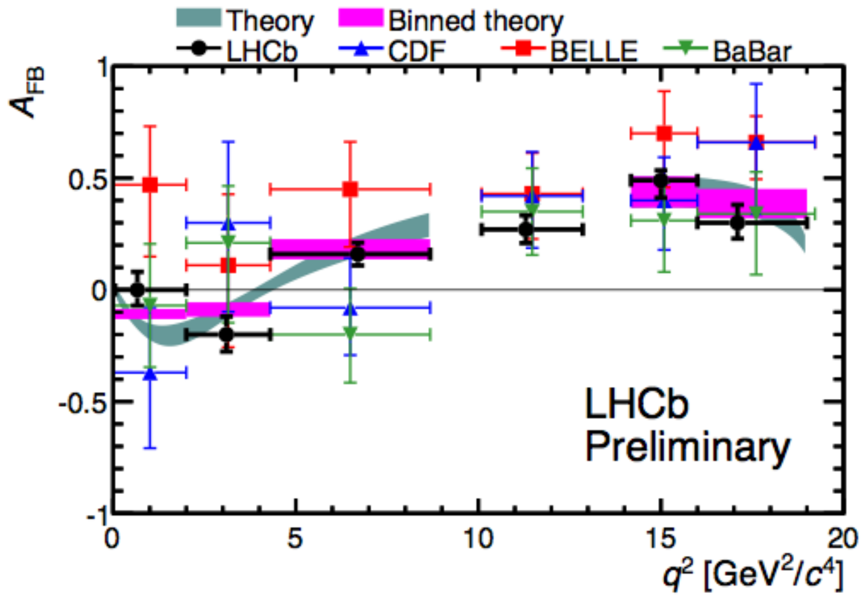

- Data points are centred at the average q^2 of events in the relevant bin, as measured from the data
- Error bars include systematic uncertainties
- Theory prediction from C. Bobeth et al. [arXiv:1105.0376] (and references therein) – no prediction in region between resonances
- Most precise measurements to-date - consistent with the SM prediction

A_{FB} zero-crossing point

LHCb-CONF-2012-008

- The zero-crossing point, q_0^2 extracted through a 2D fit to the forward- and backward-going $m_{K\pi\mu\mu}$ and q^2 distributions

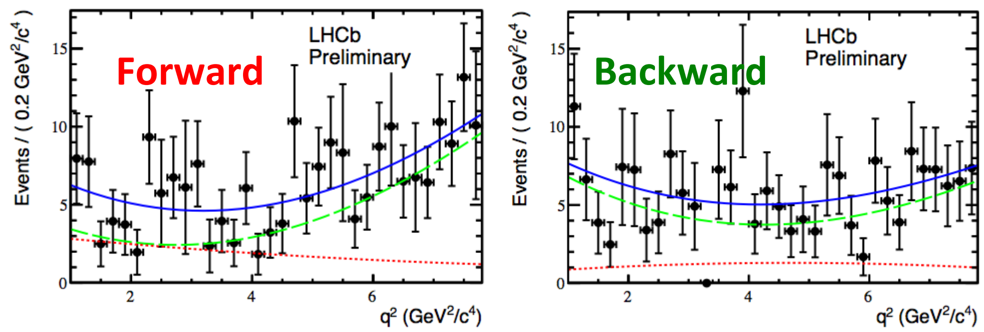

- The worlds first measurement of q_0^2, at $q_0^2 = 4.9^{+1.1}_{-1.3}$ GeV^2/c^4

- Consistent with SM prediction [arXiv:1105.0376, Eur. Phys. J. C 41 (2005) 173-188, C47 (2006) 625-641]

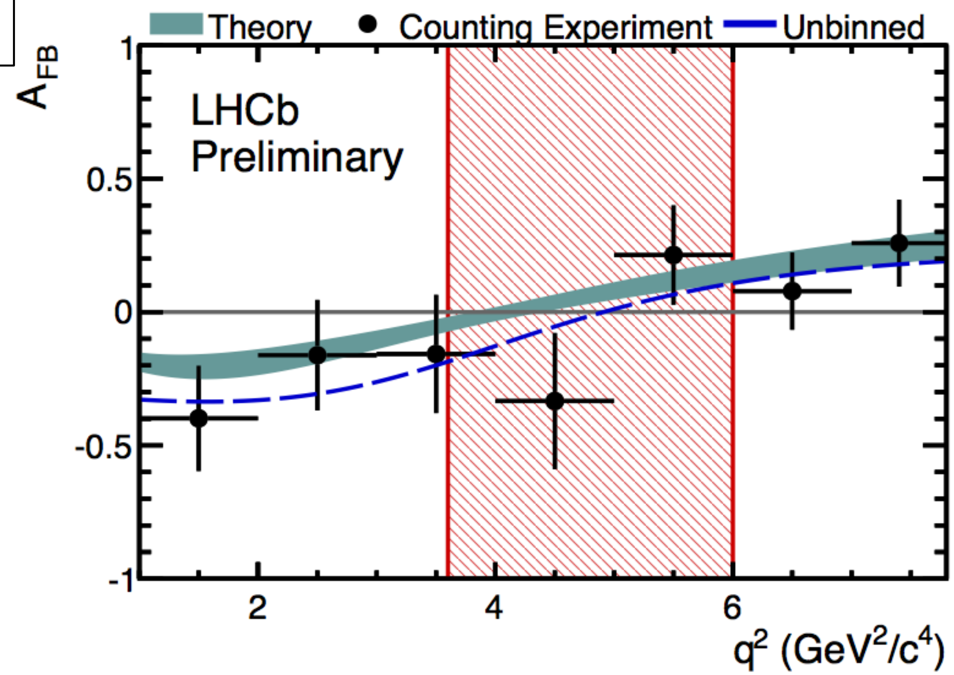

Angular Analysis Results : S_3

LHCb-CONF-2012-008

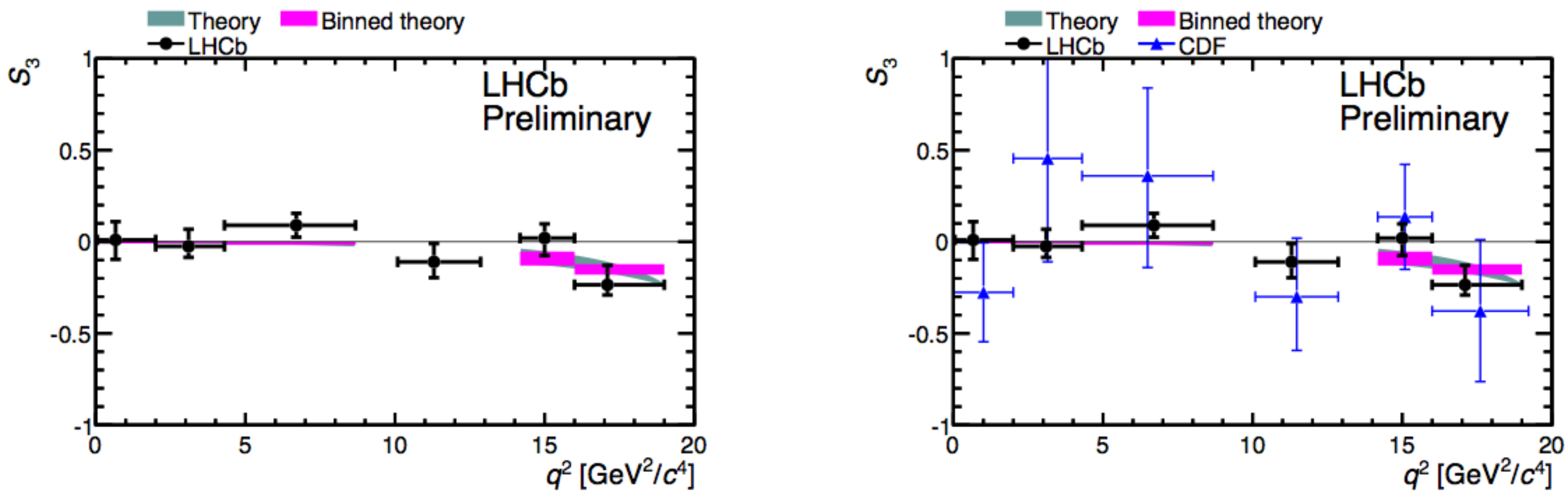

- $S_3 \propto A^2_T(1-F_L)$, the asymmetry in K^{*0} transverse polarisation

Angular Analysis Results : F_{L}, A_{Im}

LHCb-CONF-2012-008

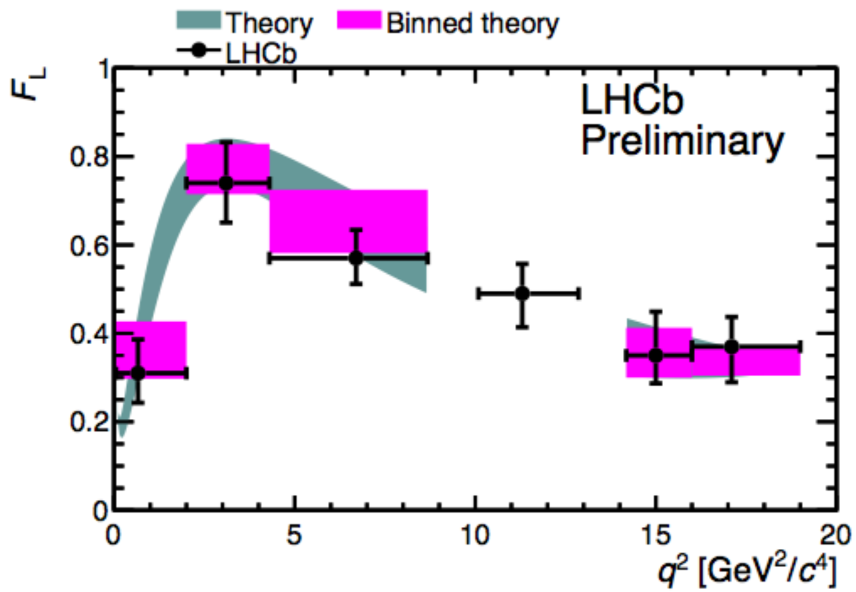

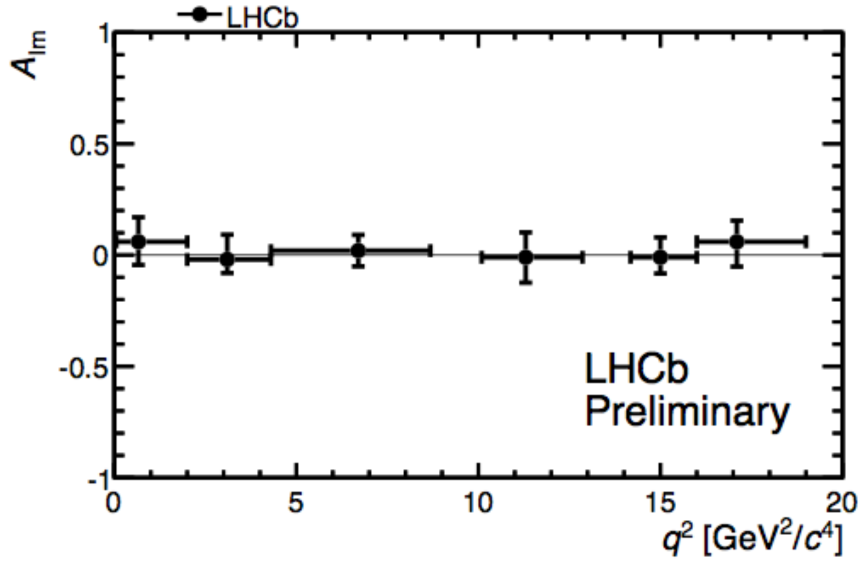

- F_L, the fraction of K^{*0} longitudinal polarisation
- A_{IM}, a T-odd CP asymmetry
- No theory prediction for A_{Im} – expected to be $O(10^{-3})$ in SM

$B^0 \to K^*\mu\mu$ and $B_s \to \phi\mu\mu$ differential BF measurements

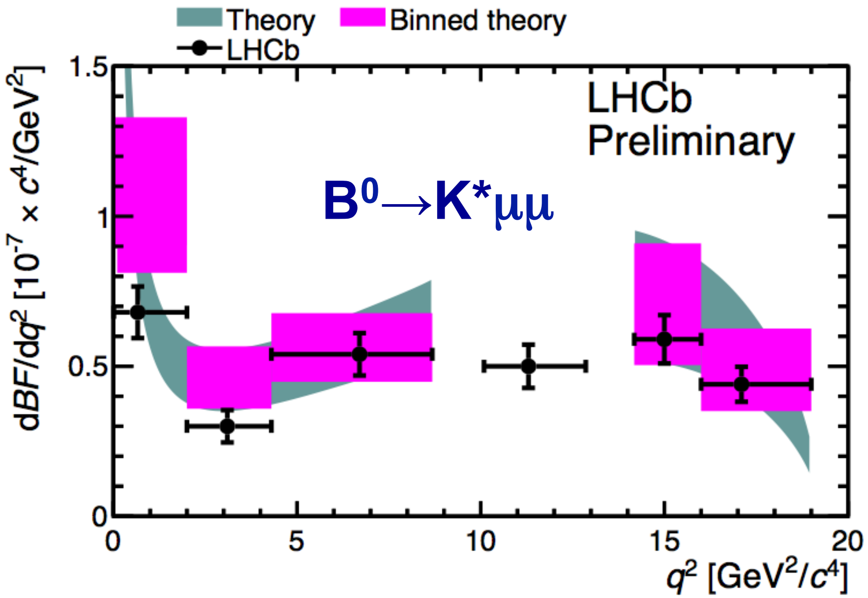

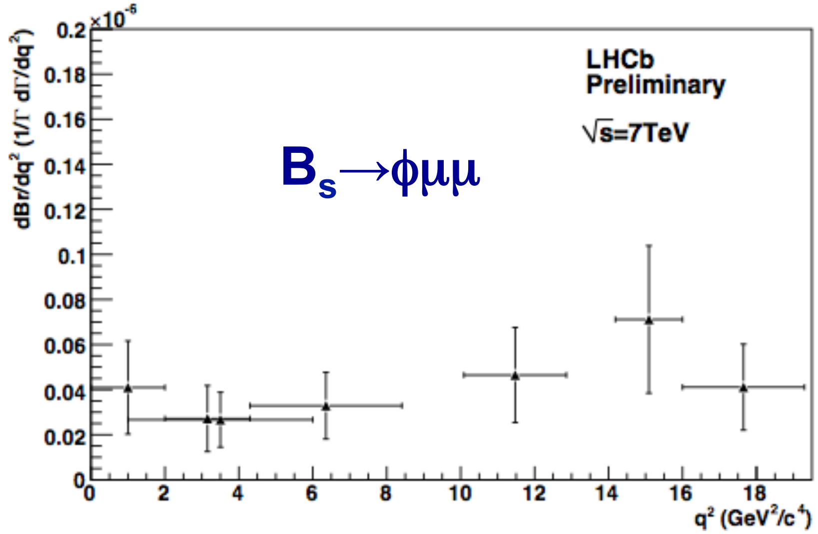

- Differential branching fraction is extracted by fitting the mass distribution and normalising to $B^0 \to K^* J/\psi$, $B_s \to \phi J/\psi$
- $B^0 \to K^*\mu\mu$: 900±34 signal events
- $B_s \to \phi\mu\mu$: 77±10 signal events
- These are the most precise measurements to-date and are consistent with SM expectations [J.Phys.G G29 (2003) 1103–1118]

LHCb-CONF-2012-008
LHCb-CONF-2012-003

Constraints on C_7, C_9, C_{10}

D. Straub, arXiv:1111.1257, JHEP 1202:106

Varying 1 Wilson coefficient at a time. $C_i = C_i^{SM} + C_i^{NP}$ *preliminary*

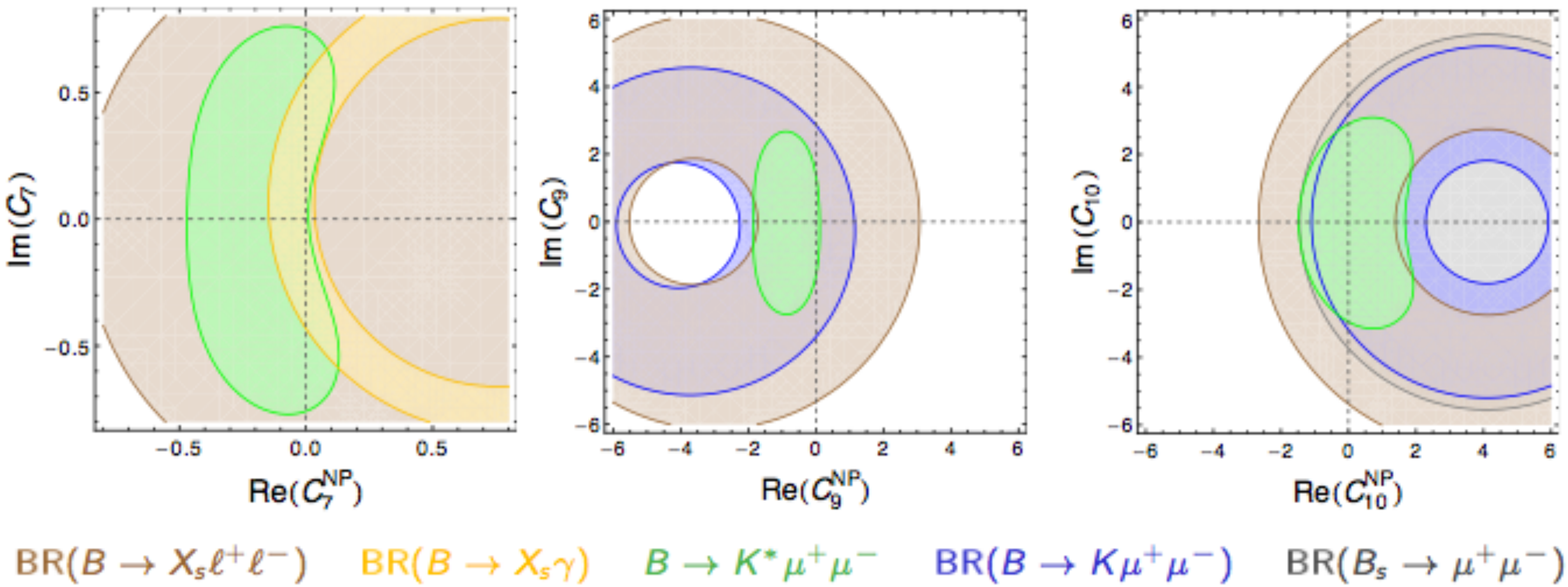

Constraints on C_7, C_9, C_{10}

D. Straub, arXiv:1111.1257, JHEP 1202:106

Varying 1 Wilson coefficient at a time. $C_i = C_i^{SM} + C_i^{NP}$ *preliminary*

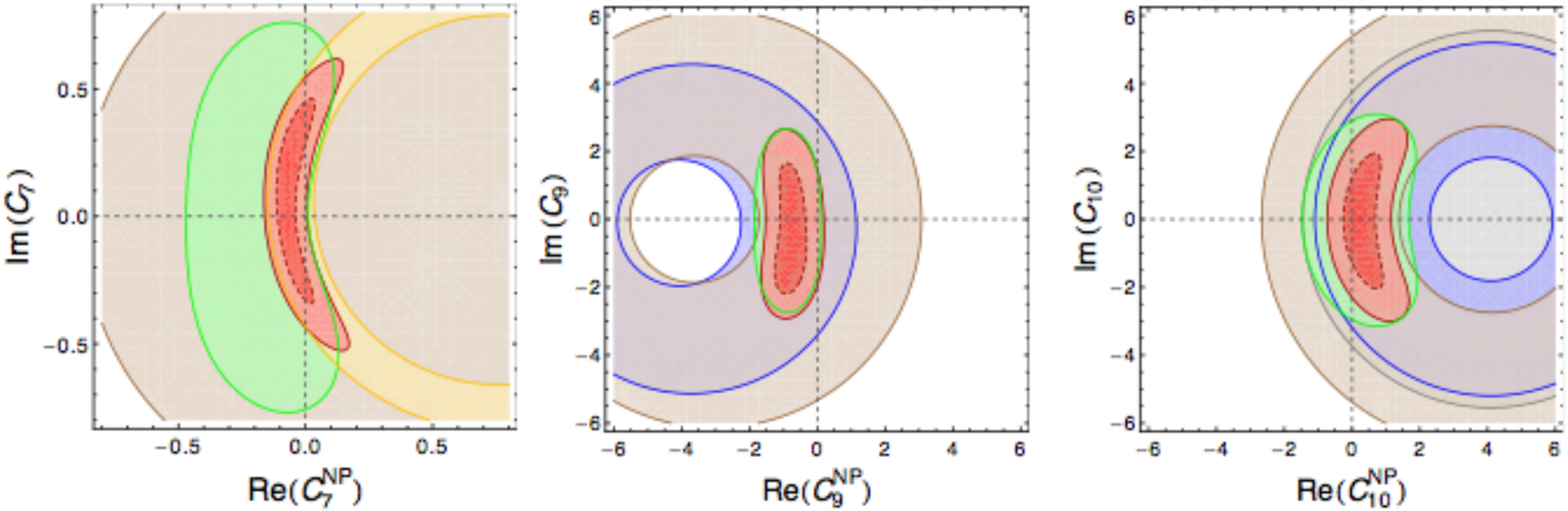

BR($B \to X_s \ell^+ \ell^-$) BR($B \to X_s \gamma$) $B \to K^* \mu^+ \mu^-$ BR($B \to K \mu^+ \mu^-$) BR($B_s \to \mu^+ \mu^-$)

- Good agreement with SM expectations
- Complementarity between observables crucial to break degeneracies

Impact – with tree level FV

D. Straub, arXiv:1111.1257, JHEP 1202:106

Results can be interpreted as bounds on the scale of new physics:

$$\mathscr{L} = \mathscr{L}_{\mathrm{SM}} + \sum_{j=7,9,10} \frac{e^{i\phi_j}}{\Lambda_j^2} \mathcal{O}_j$$

~tree level generic flavour violation

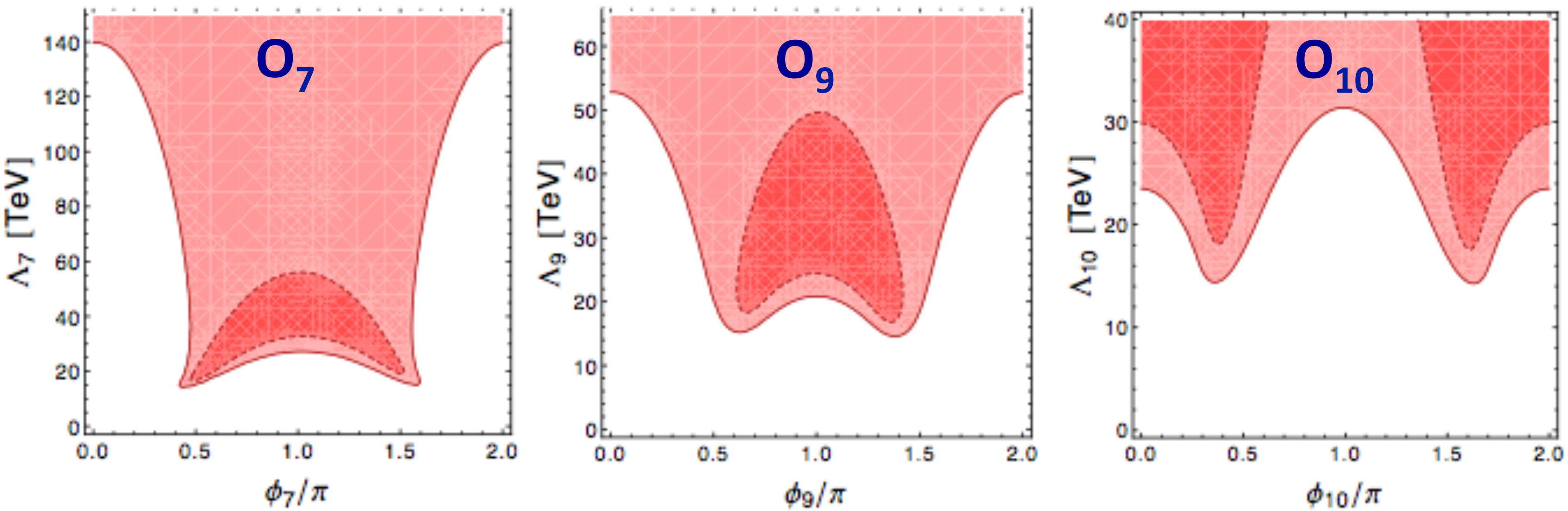

Impact – with loop CKM-like FV

D. Straub, arXiv:1111.1257, JHEP 1202:106

Results can be interpreted as bounds on the scale of new physics:

$$\mathscr{L} = \mathscr{L}_{SM} - \sum_{j=7,9,10} \frac{V_{tb}V_{ts}^*}{16\pi^2} \frac{e^{i\phi_j}}{\Lambda_j^2} \mathcal{O}_j$$

~loop level CKM-like flavour violation

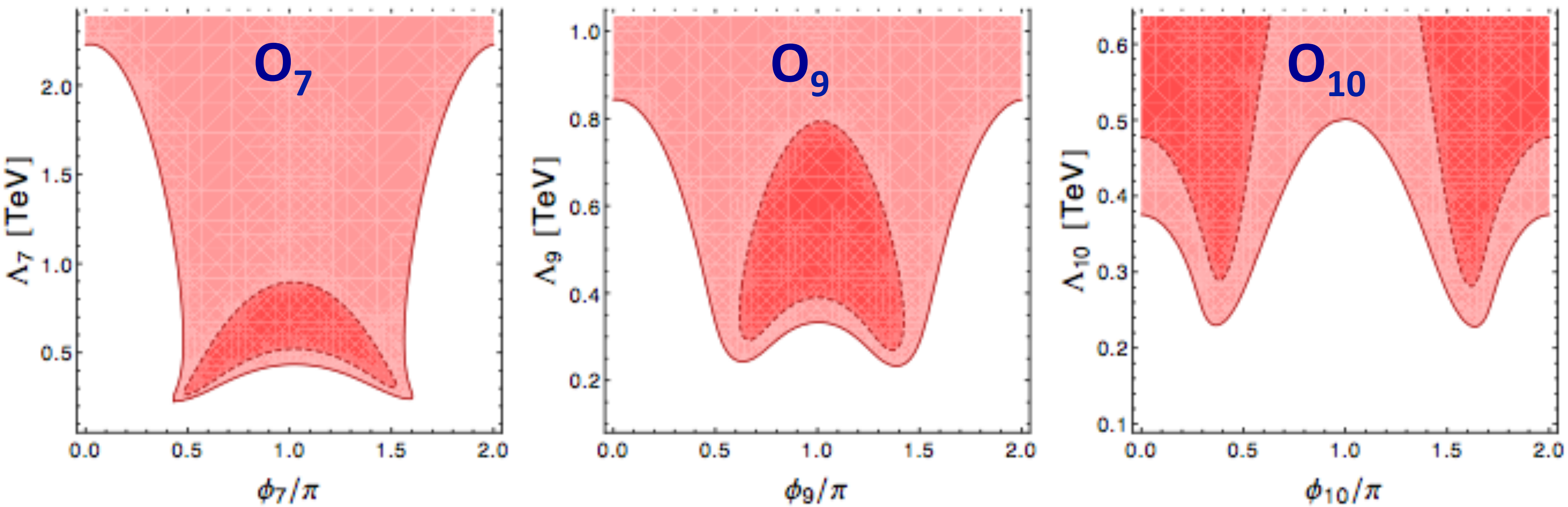

- Bounds are weaker in the presence of CP violation beyond the CKM
- Reason: only CP-averaged observables
- Measurement of CP asymmetries would be welcome

$B^0 \to K^* \mu\mu$ – Outlook

- Measurement of $B^0 \to K^* \mu\mu$ CP asymmetry in progress

- More data will enable a full angular fit to extract complete information from $B^0 \to K^* \mu\mu$ decays

  → host of theoretically well calculable observables

- Angular analysis of $B^+ \to K^+ \mu\mu$ decays also in progress

CP-averaged angular coeff.

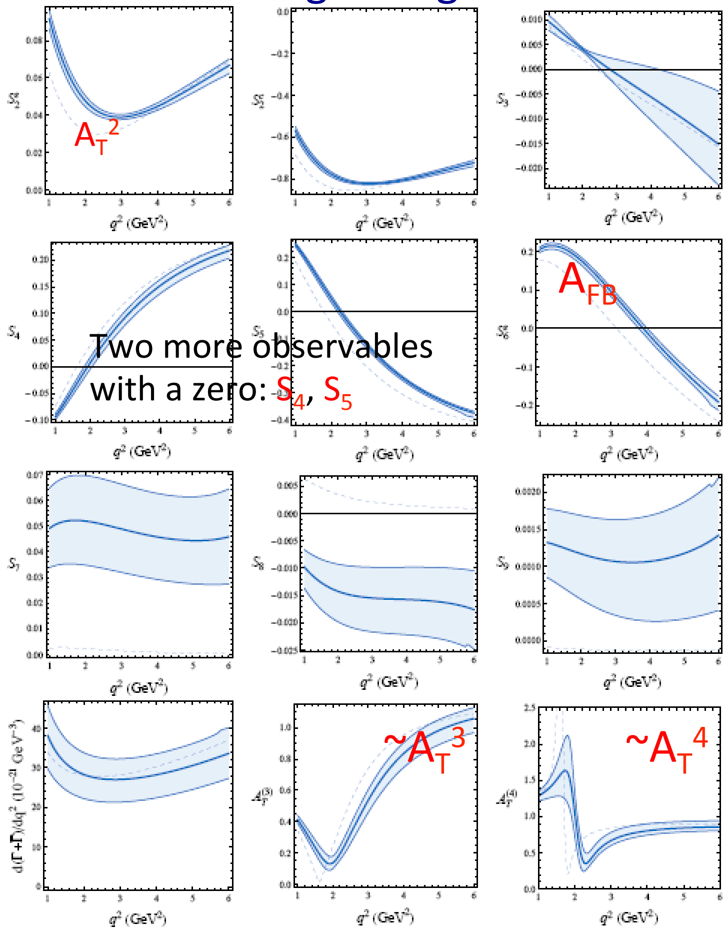

W.Altmannshofer et. al. [arXiv:0801.1214]

The search for $B^+ \rightarrow \pi^+ \mu^+ \mu^-$

The search for $B^+ \to \pi^+\mu^+\mu^-$

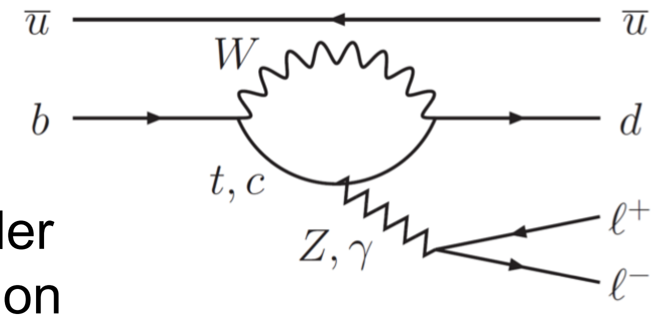

- The $B^+ \to \pi^+\mu^+\mu^-$ decay is a $b \to d$ transition
- In the SM the branching fraction is ~25x smaller than the well known $B^+ \to K^+\mu^+\mu^-$ ($b \to s$) transition and can be enhanced in new physics models
- SM prediction: $\mathcal{B}(B^+ \to \pi^+\mu^+\mu^-) = (1.96 \pm 0.21) \times 10^{-8}$ (*)
- Previous best limit from Belle: $\mathcal{B}(B^+ \to \pi^+\mu^+\mu^-) < 6.9 \times 10^{-8}$ (90% CL) (**)
- While ratio CKM elements V_{ts}/V_{td} known from oscillation measurements, this decay probes V_{ts}/V_{td} in above penguin decays
- Measure branching fraction to determine coupling

(*) Hai-Zhen et al., Comm in Theo Ph 50 (2008) 696
(**) J.T. Wei et al., Phys. Rev. D78 (2008) 011101

Motivation – tension in the CKM picture

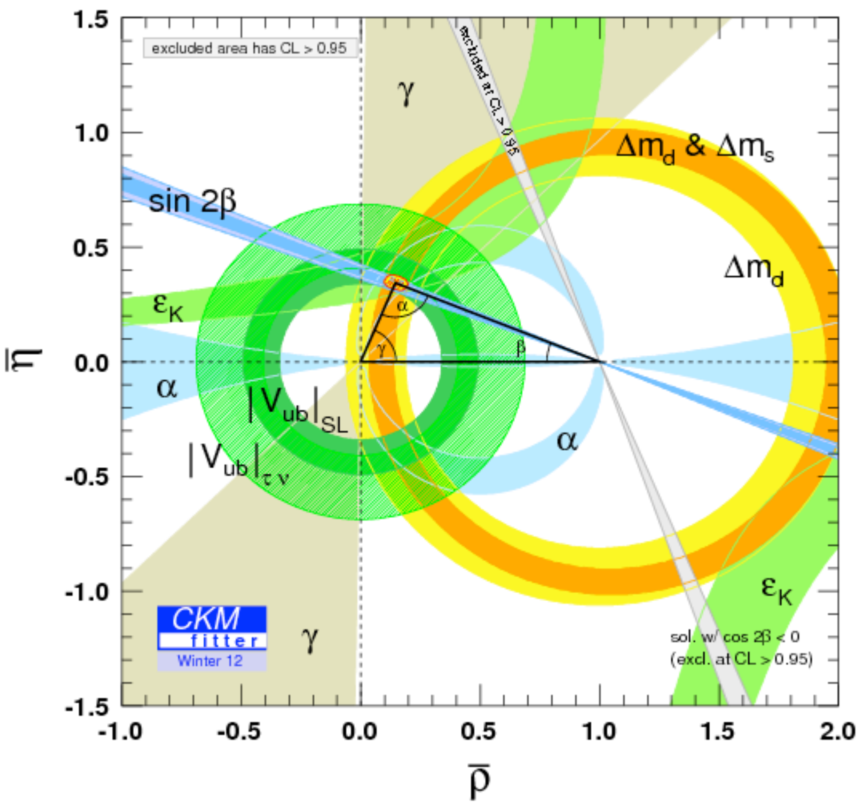

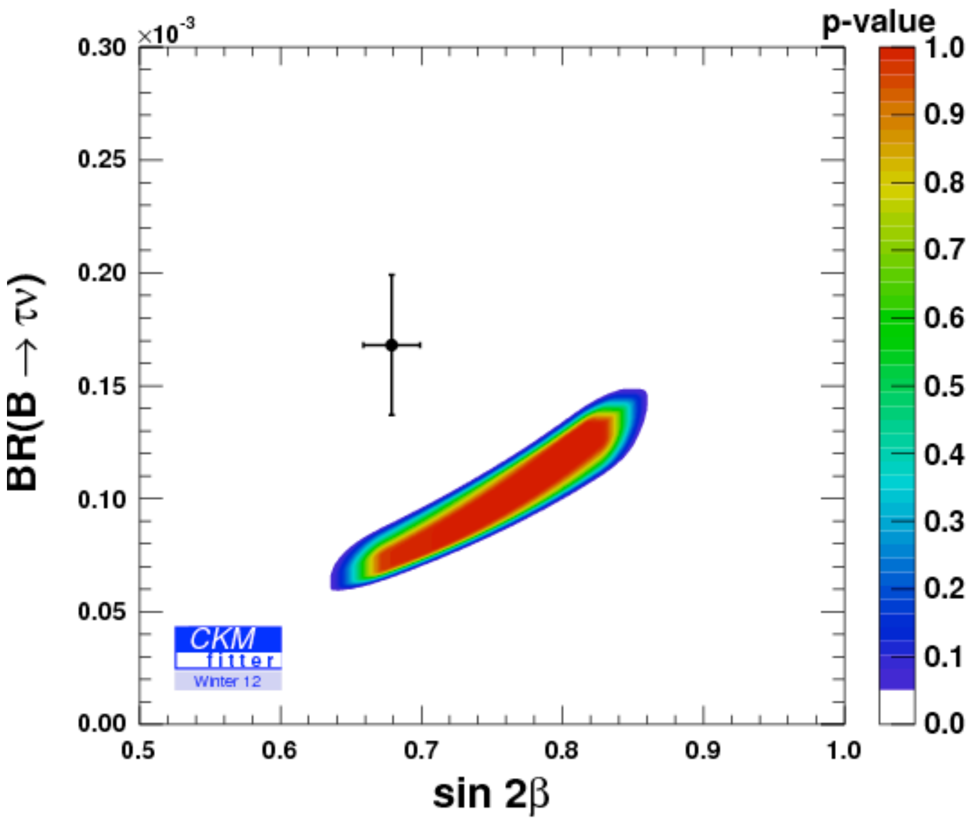

- Tension between sin 2β and $Vub|_{B\to\tau\nu}$ measurements and global fit
- Information from comparing angle to opposite side
- LHCb will improve measurement angle γ → alternative measurements of Vts/Vtd also of interest

$B^+ \to \pi^+\mu^+\mu^-$ Analysis

- Main issue: separating $B^+ \to \pi^+\mu^+\mu^-$ from misidentified $B^+ \to K^+\mu^+\mu^-$

- Use BDT to make selection:
  - kinematic properties of the B candidate and daughters
  - particle identification information handled separately
  - $B^+ \to (J/\psi, \Psi(2S))K^+$ vetoes
  - peaking backgrounds negligible

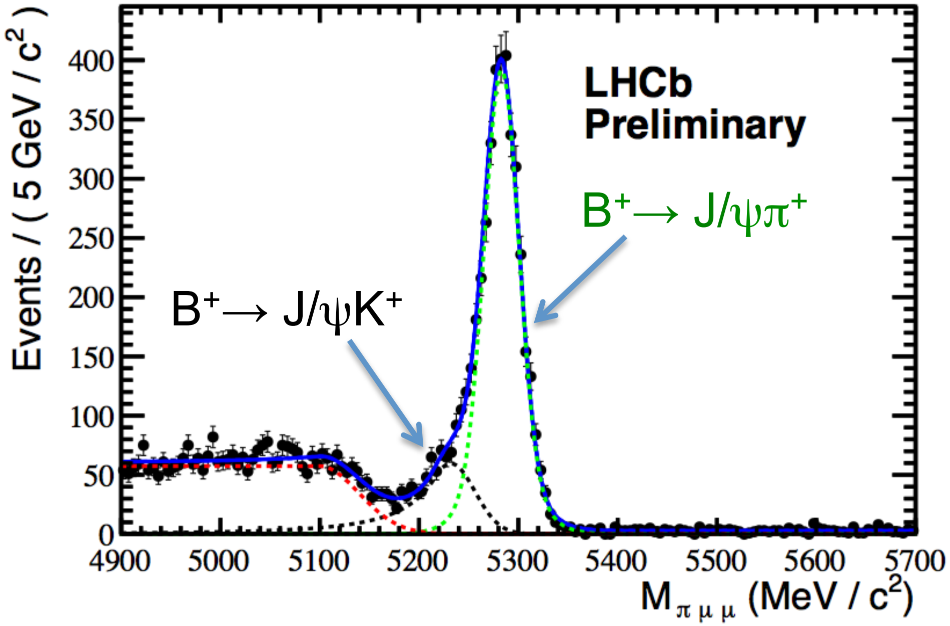

- Fitting
  - Use $B^+ \to J/\psi K^+$ events to define signal shape and, under $\pi^+\mu^+\mu^-$ hypothesis, shape of mis-identified events
  - Components for partial reconstructed B decays and combinatorial bkgrd
  - Validate by separating $B^+ \to J/\psi K^+$ and $B^+ \to J/\psi\pi^+$ decays
  - Normalise branching fraction using $B^+ \to J/\psi K^+$

Result

- With 1.0 fb^{-1} LHCb finds $25.3^{+6.7}_{-6.4}$ $B^+ \to \pi^+\mu^+\mu^-$ signal events
  - 5.2σ excess above background

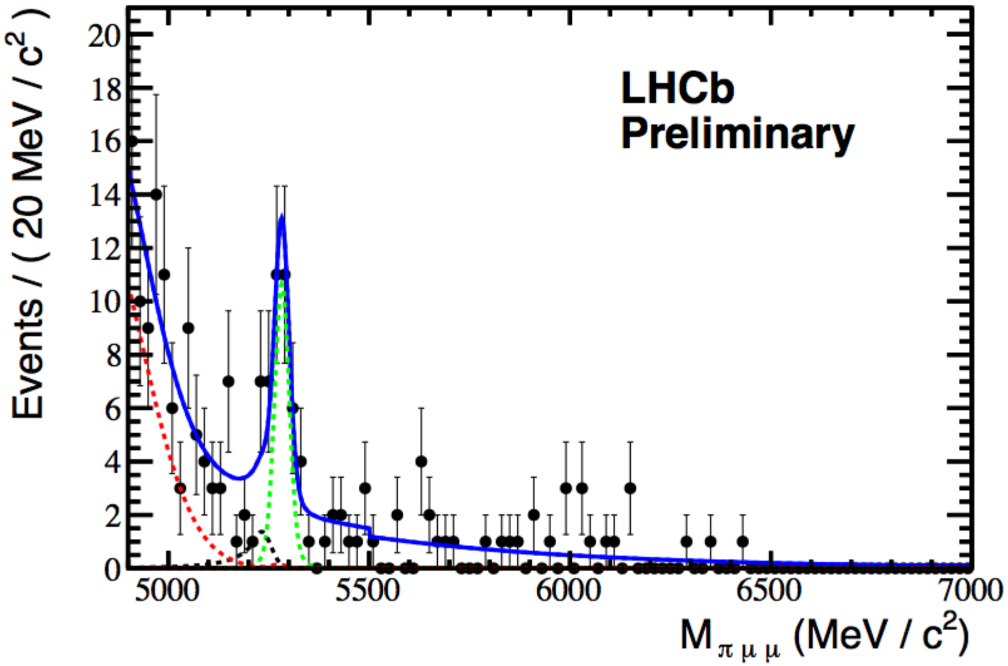

[LHCb-CONF-2012-006]

- $B(B^+ \to \pi^+\mu^+\mu^-) = (2.4 \pm 0.6(stat) \pm 0.2(syst)) \times 10^{-8}$, within 1σ of SM pred.
- The rarest B decay ever observed

Isospin Asymmetry in $B \to K^{(*)}\mu^+\mu^-$

- Results shown in public for first time
- Will shortly be available in LHCb paper : LHCb-PAPER-2012-011

Isospin Asymmetry

- The isospin asymmetry of $B \rightarrow K^{(*)}\mu^+\mu^-$, A_I is defined as:

$$A_I = \frac{\mathcal{B}(B^0 \to K^{(*)0}\mu^+\mu^-) - \frac{\tau_0}{\tau_+}\mathcal{B}(B^\pm \to K^{(*)\pm}\mu^+\mu^-)}{\mathcal{B}(B^0 \to K^{(*)0}\mu^+\mu^-) + \frac{\tau_0}{\tau_+}\mathcal{B}(B^\pm \to K^{(*)\pm}\mu^+\mu^-)}$$

can be more precisely predicted than the branching fractions

- A_I is expected to be very close to zero in the SM e.g. for $B \rightarrow K^*\mu^+\mu^-$:

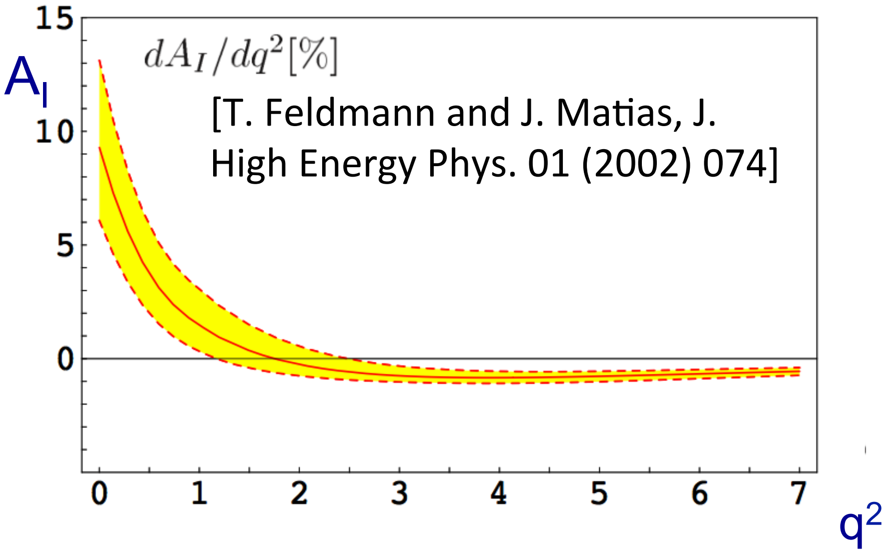

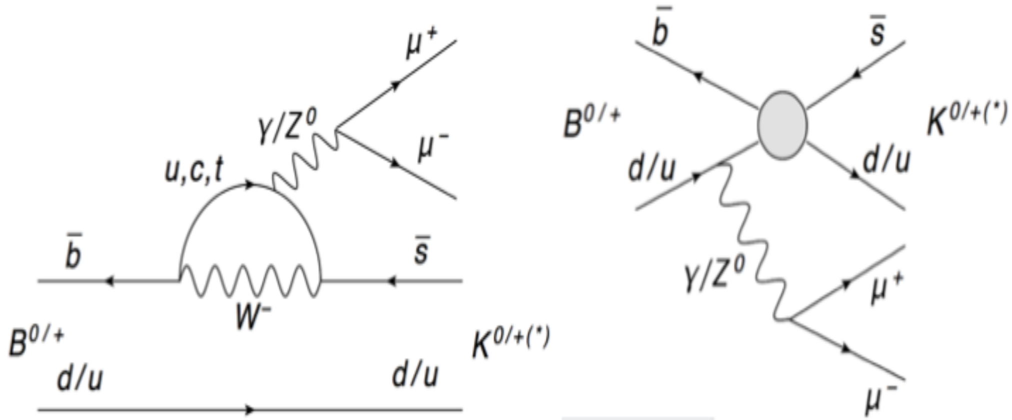

- Asymmetry has been measured in $K^*\gamma$ decay modes, agrees with SM

Experimental Status

- CDF, Belle and Babar have all measured A_I :

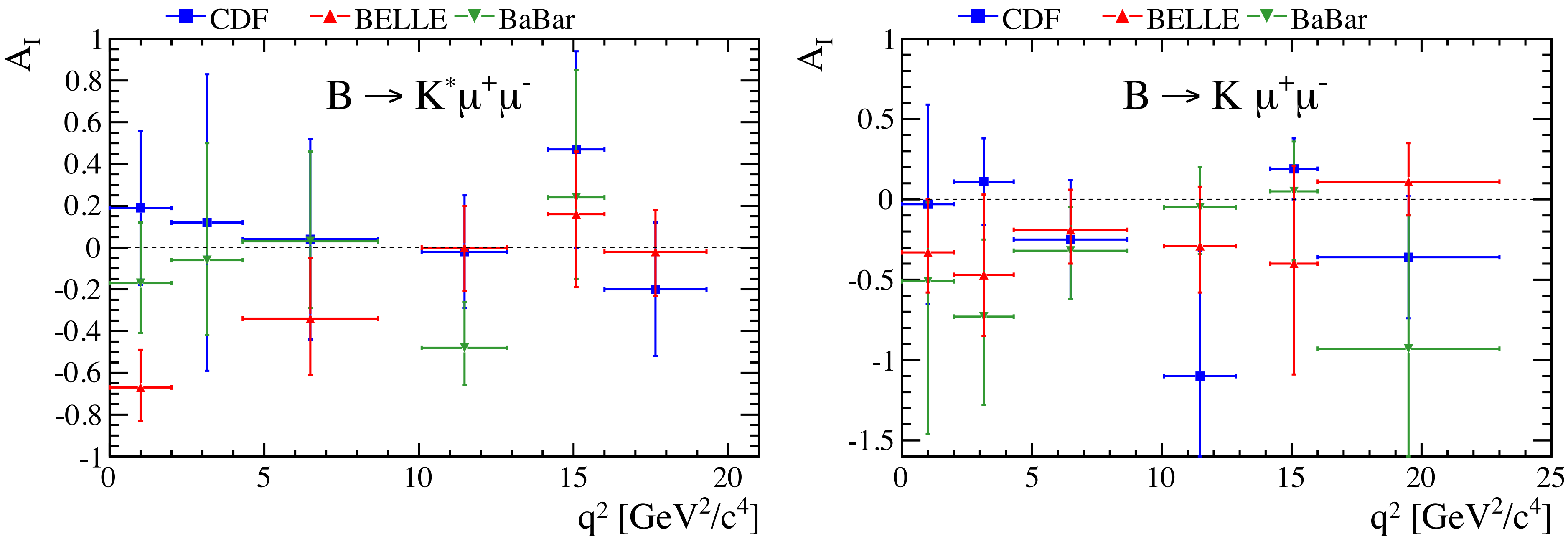

- For $B \to K^* \mu^+ \mu^-$ results are consistent with the SM
- There is still some tension for $B \to K \mu^+ \mu^-$
- Deficit in $K_S \mu\mu$ events → large negative A_I (with large uncertainty)

[B. Aubert et al., submitted to Phys. Rev. D, arXiv:1204.3933]
[J.-T. Wei et al. Phys. Rev. Lett. 103 (2009) 171801, arXiv:0804.4770]
[CDF, Phys.Rev.Lett. 107 (2011) 201802, arXiv:1204.3933]

Experimental Status

Babar, Phys. Rev. Lett. 102 (2008) 091803, arXiv:0807.4119

- CDF, Belle

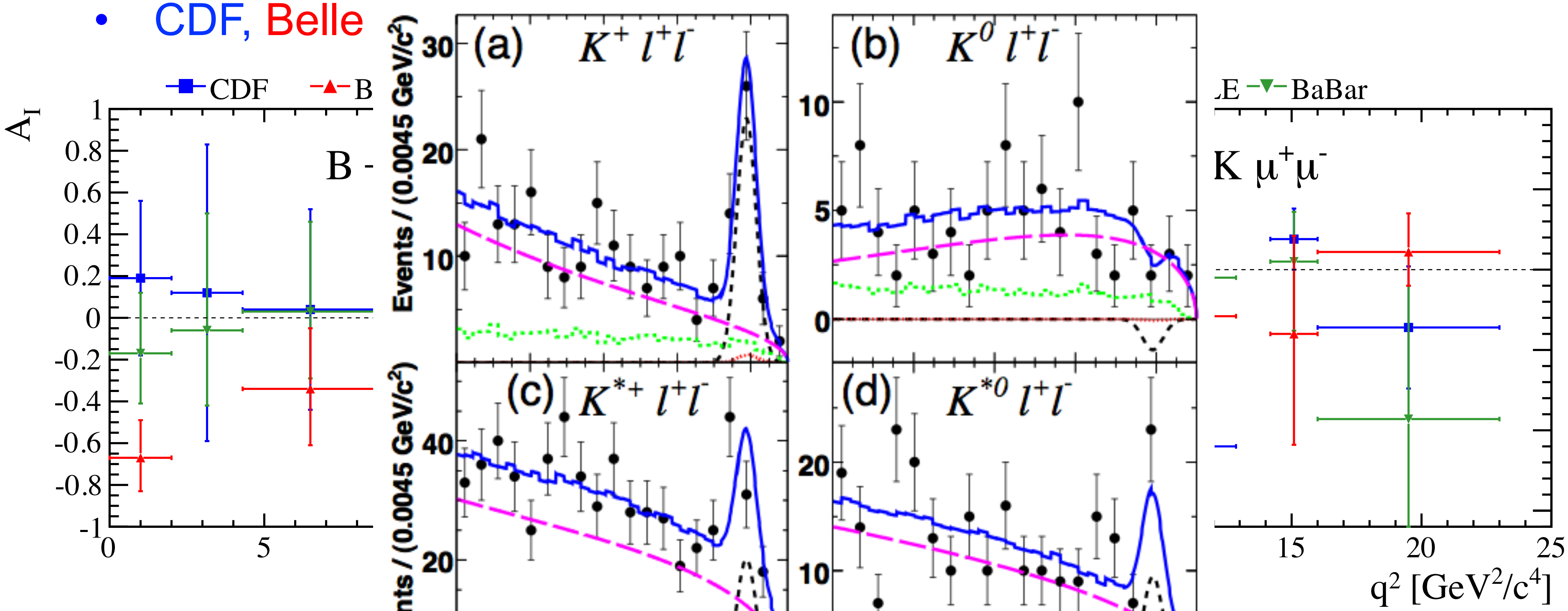

- For B→K*μ
- There is sti
- Deficit in $K_S\mu\mu$ events → large negative A_I (with large uncertainty)

ubert et al., submitted to Phys. D, arXiv:1204.3933]
. Wei et al. Phys. Rev. Lett. 103 9) 171801, arXiv:0804.4770]
[CDF, Phys.Rev.Lett. 107 (2011) 201802, arXiv:1204.3933]

LHCb Analysis

- Measure differential branching fraction of four decay modes:
  - $B^+ \to (K^{*+} \to K_S^0 \pi^+) \mu^+ \mu^-$
  - $B^0 \to (K^0 \to K_S^0) \mu^+ \mu^-$
  - $B^0 \to K^{*0} \mu^+ \mu^-$
  - $B^+ \to K^+ \mu^+ \mu^-$
- K_S^0 are reconstructed through the $K_S^0 \to \pi^+ \pi^-$ decay mode
- The K^{*+} and K_S^0 channels have a lower reconstruction efficiency and a lower visible branching fraction
- The K^{*0} and K^+ channels much more copious

Preliminary

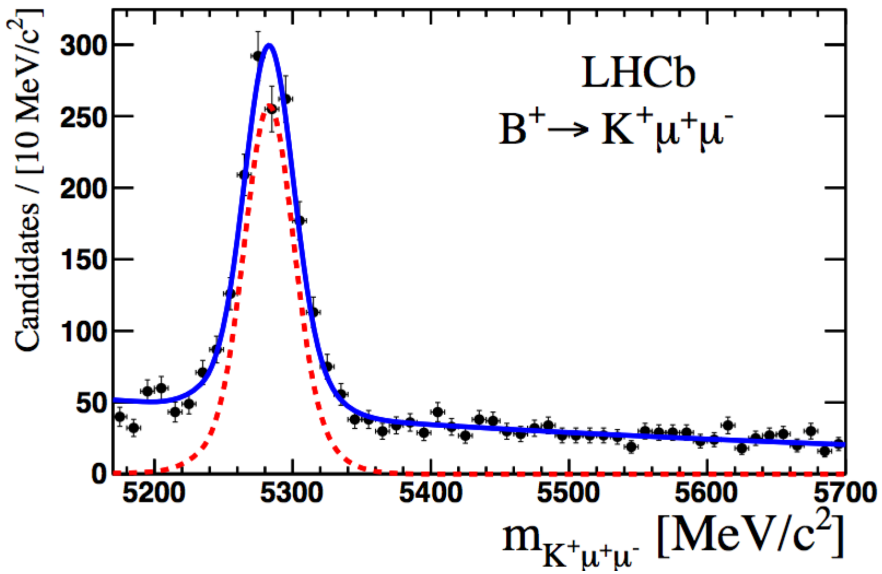

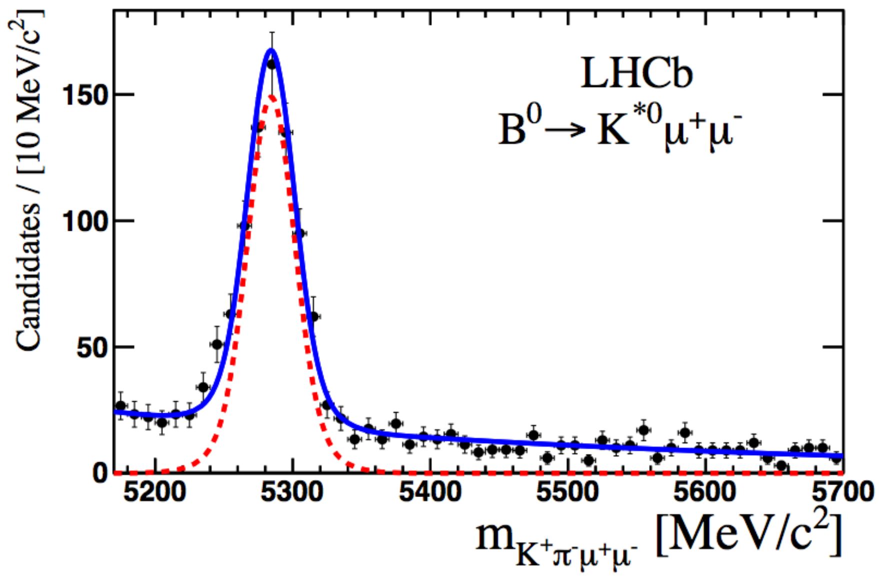

LHCb Analysis

- The channels involving a K_S^0 are split into two categories based on how the K_S^0 is reconstructed – "long" (L) and "downstream" (D)
  - L-events have less background – use cut-based selection
  - D-events – use BDT selection
  - Insofar as possible, use similar selections for K^+ channels

- Correction for detector and selection effects again made with simulation (verified to reproduce the data)

- $B \to K^{(*)}(J/\psi \to \mu^+\mu^-)$ decays are used to normalise branching fraction for each decay to cancel systematic uncertainties

- Determine A_I by combining the likelihoods of the relevant decay modes

$B(B^+ \to K^{*+}\mu^+\mu^-)$

- LHCb measurement: $B(B^+ \to K^{*+}\mu^+\mu^-) = (1.16 \pm 0.19) \times 10^{-6}$
- Cf. PDG $B(B^+ \to K^{*+}\mu^+\mu^-) = (1.16 \pm 0.30) \times 10^{-6}$

Preliminary

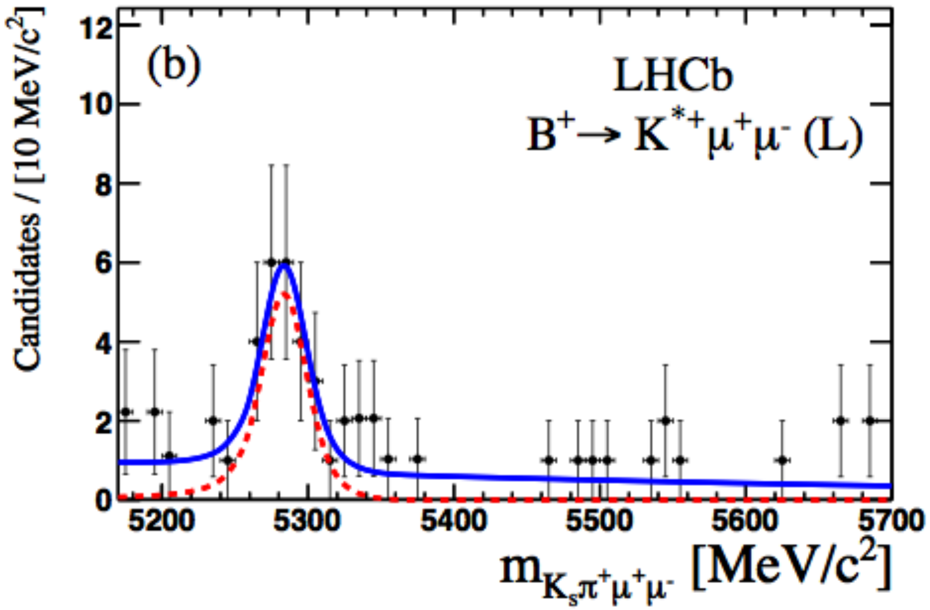

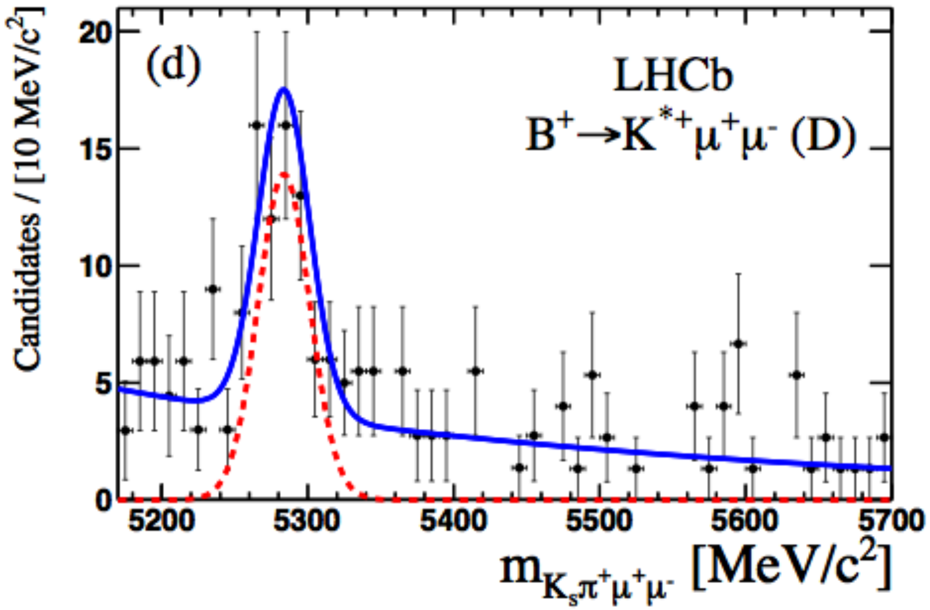

$dBF/q^2(B^+ \rightarrow K^{*+}\mu^+\mu^-)$

- Measurements are consistent with the SM :

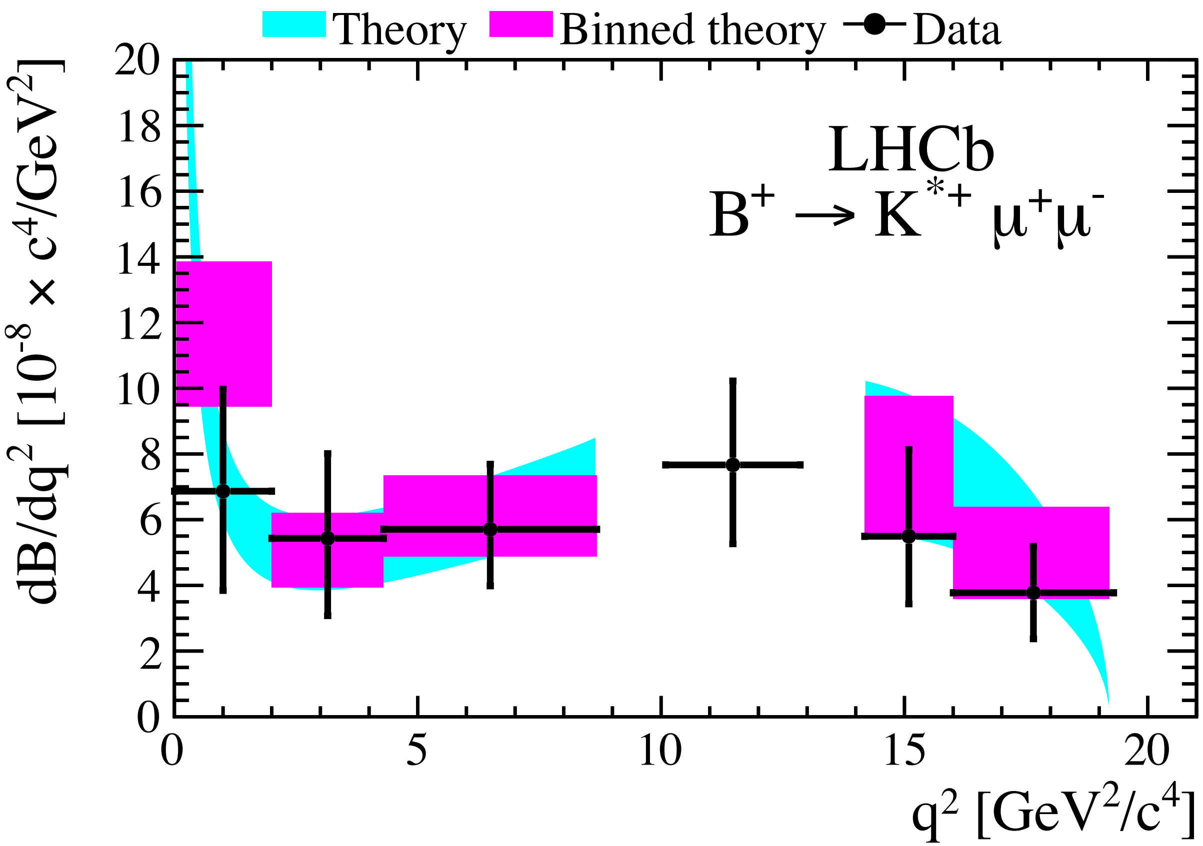

Preliminary

Theory prediction from [C. Bobeth, G. Hiller, and D. van Dyk, JHEP (2011) 067, arXiv:1105.0376]

A_I for $B \to K^* \mu^+ \mu^-$

- A_I for $B \to K^* \mu^+ \mu^-$ is consistent with zero, as predicted by the SM
- LHCb results in agreement with previous measurements

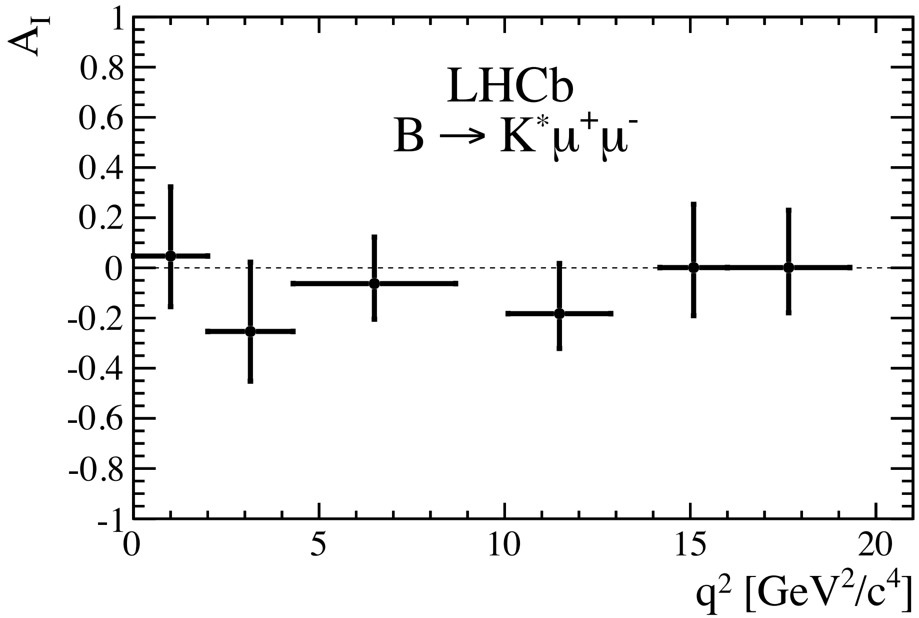

Preliminary

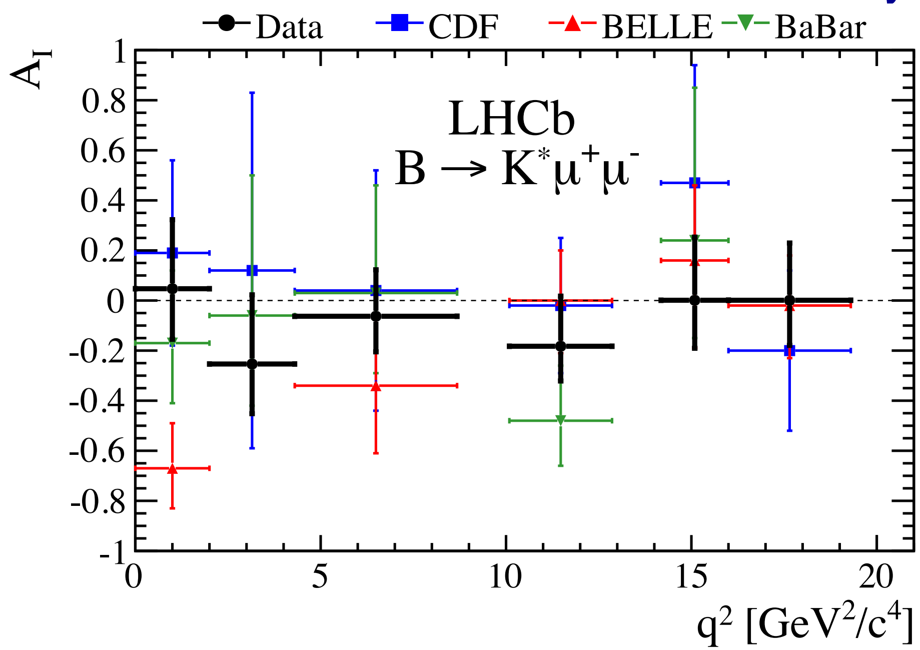

$B(B^0 \to K^0 \mu^+ \mu^-)$

- Assuming a factor two for $K^0 \to K^0_S$ and accounting for $K_S^0 \to \pi^+\pi^-$ branching fraction :
- LHCb measurement: $B(B^0 \to K^0\mu^+\mu^-) = (3.1^{+0.7}_{-0.6})\times10^{-7}$
- cf PDG $B(B^0 \to K^0\mu^+\mu^-) = (4.5\pm1.1)\times10^{-7}$

  $B(B^0 \to K^0 l^+ l^-) = (3.1^{+0.8}_{-0.7})\times10^{-7}$
- 5.7σ excess above background

Preliminary

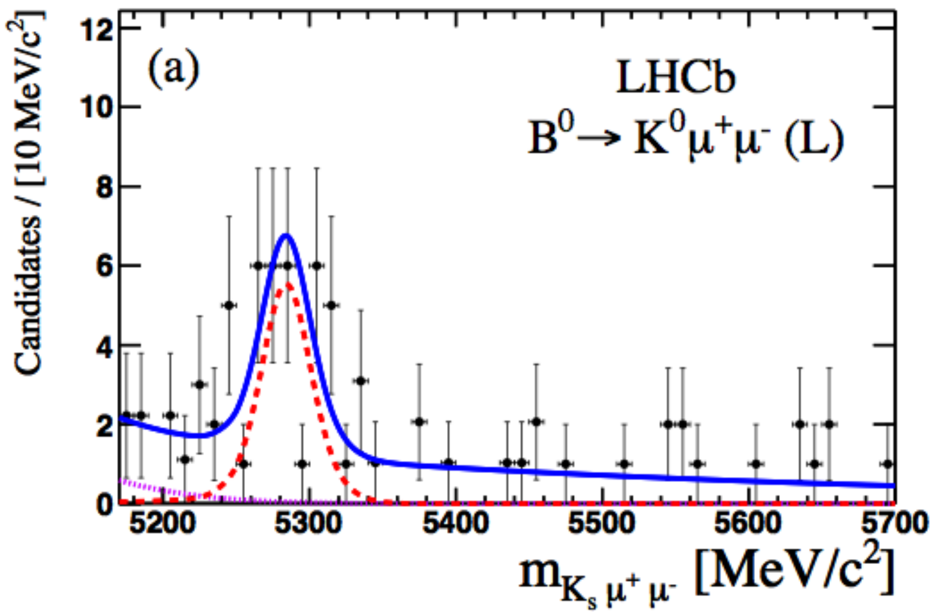

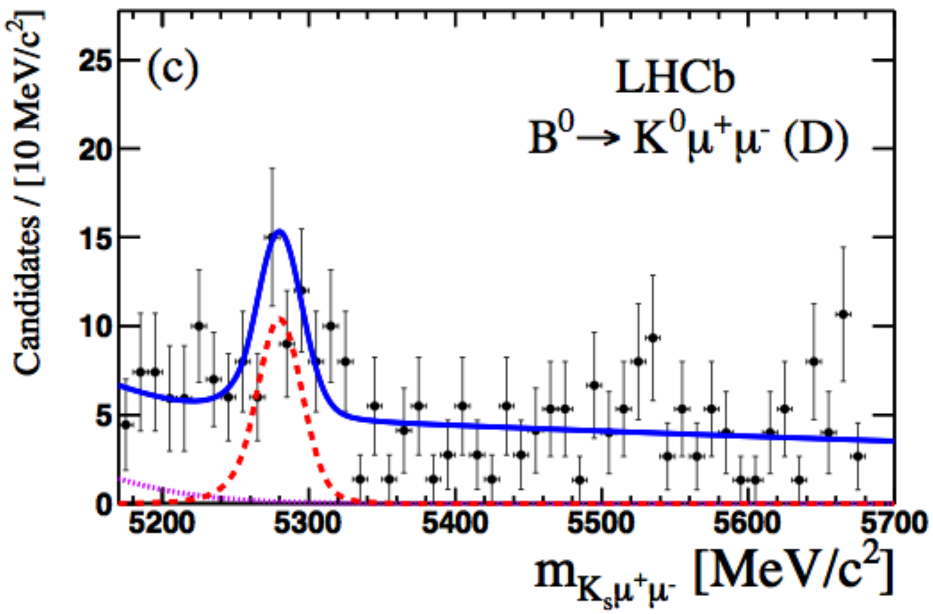

dBF/q^2($B^0 \to K^0 \mu^+ \mu^-$)

- There is a deficit of $B^0 \to K^0 \mu^+ \mu^-$ signal in the q^2 regions which are not adjacent to the charmonium resonances

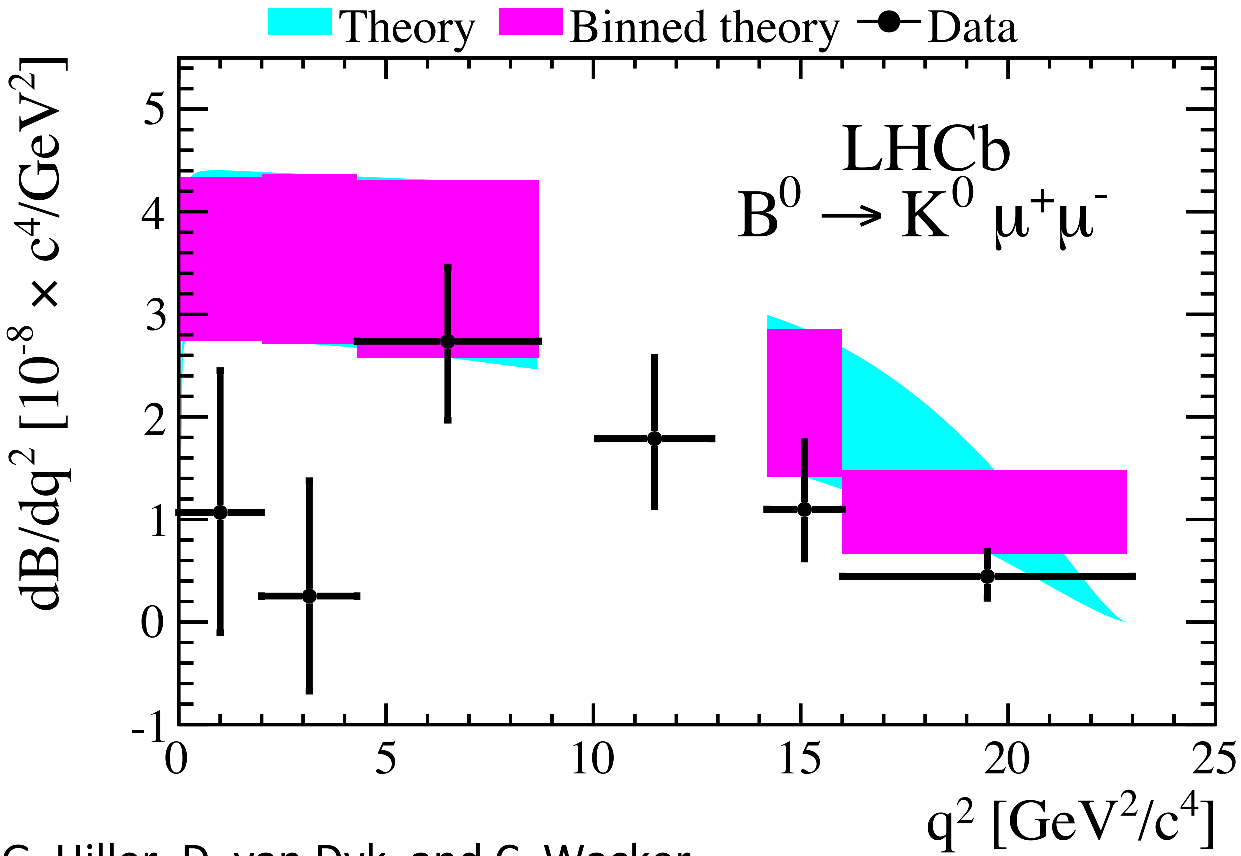

Preliminary

C. Bobeth, G. Hiller, D. van Dyk, and C. Wacker, JHEP 1201 (2012) 107, arXiv:1111.2558.

A_I for $B \to K\mu^+\mu^-$

- As a result, A_I for $B \to K\mu^+\mu^-$ tends to sit below the SM prediction
- Results agree with previous measurements but nearly all measurements of A_I are negative
- Ignoring the small correlation of (syst) errors between each q^2 bin, the significance of the deviation from zero integrated across q^2 is 4.4σ (from LHCb alone)

Preliminary

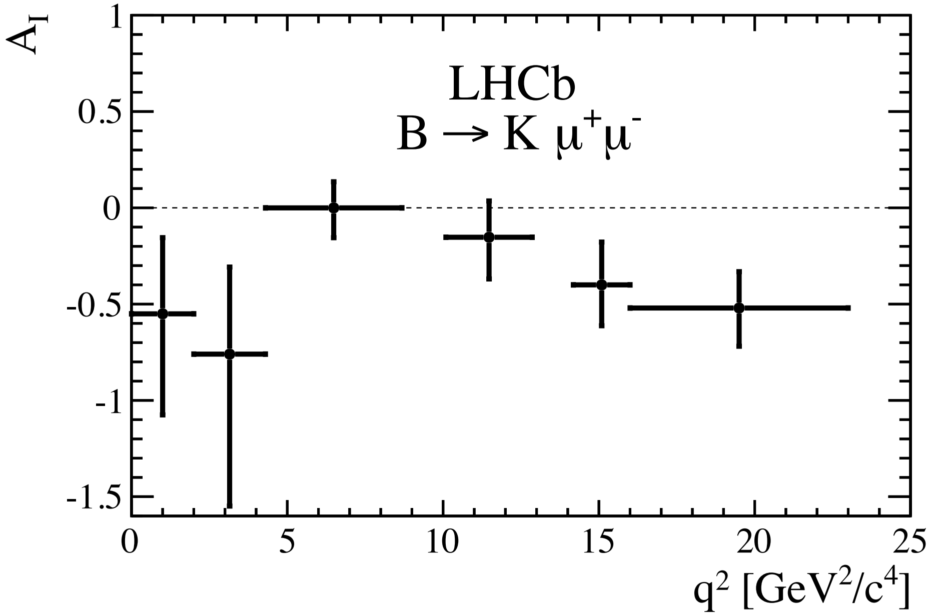

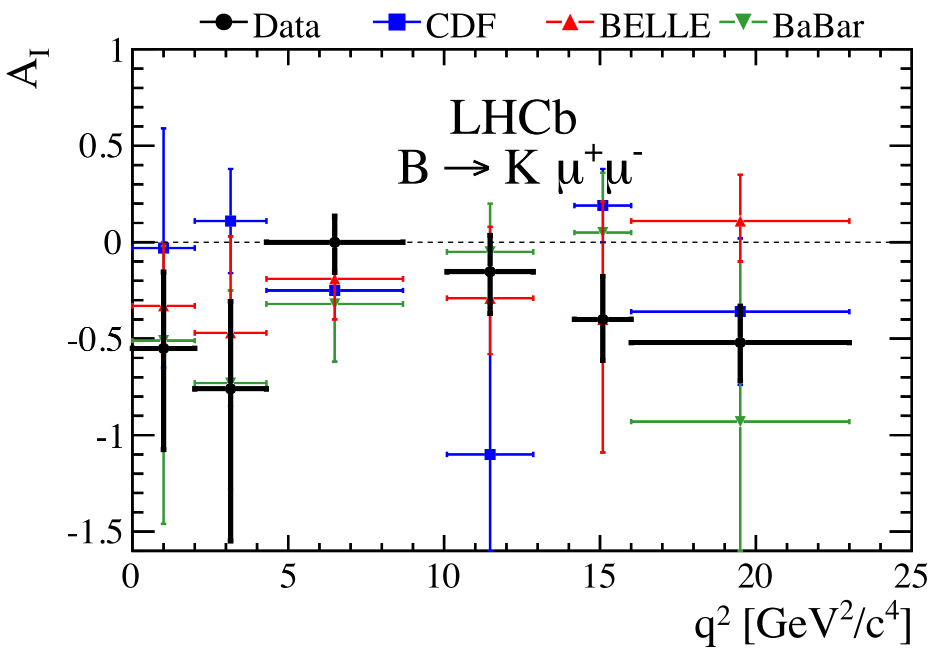

Cross checks

- Hard to imagine some expt'al issue that effects the K^0 decays but not the $K^{*+}(\rightarrow K^0\pi^+)$
- Normalise BF to $J/\psi K^+$ and $J/\psi K^0$ – is only the shape of the relative efficiency that the measurement is sensitive to
  - Most significant effect seen in A_I is at high q^2 – where efficiency is very close to that in J/ψ regions
  - At low q^2, harder K_S^0, longer flight distance, decay beyond tracking stations and are not reconstructed – essentially geometry

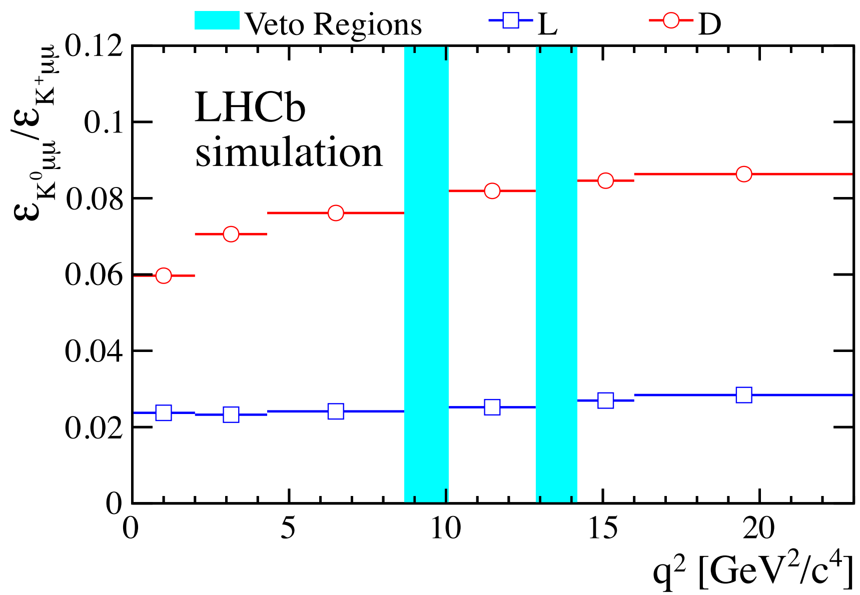

$A_{CP}(B^0 \to K^*\gamma)$

$A_{CP}(B^0 \to K^*\gamma)$

- CLEO's 10 events in 1993 → LHCb's 5300 in 2011
  - Can expect another two orders of magnitude increase in the next decade with LHCb upgrade
- Probe CP violation in $b \to s\gamma$ via the exclusive mode $B^0 \to K^*\gamma$
  - SM prediction: A_{CP} = -0.006 ± 0.004

    (Previous best measurement: A_{CP} = -0.016 ± 0.022 ± 0.007 [BaBar])
- Fit for raw asymmetry
  - Subtract B^0 production asymmetry, $K\pi$ detection asymmetry
- **A_{CP} ($B^0 \to K^*\gamma$) = -0.008 ± 0.017 (stat) ± 0.009 (syst)**

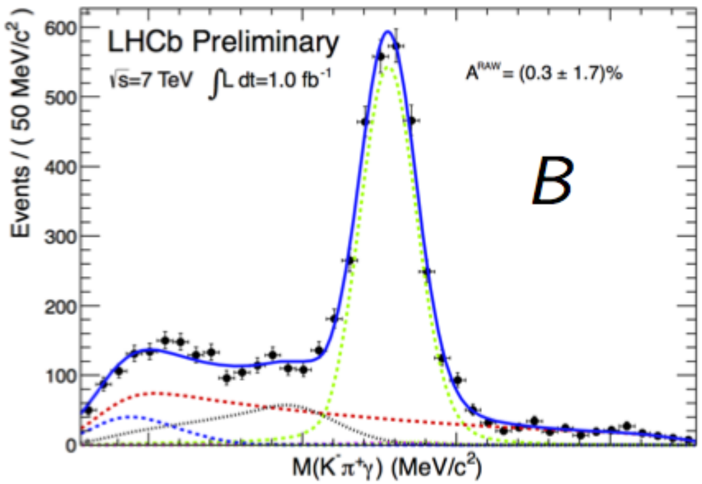

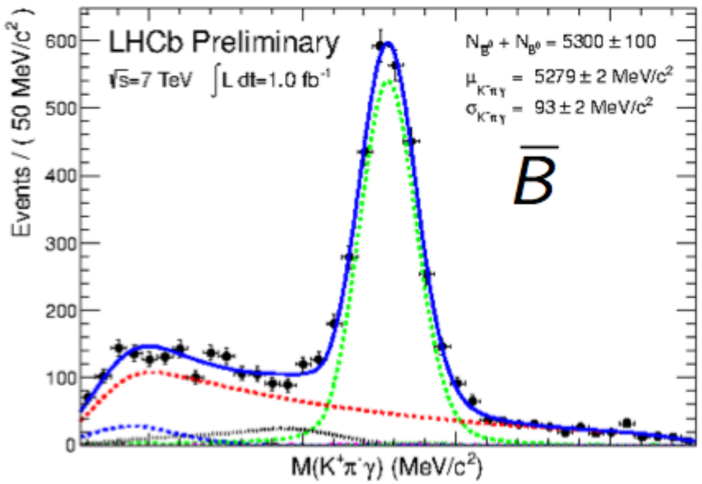

Conclusions

- World's most precise measurements of angular observables and differential branching fraction in $B^0 \to K^* \mu^+ \mu^-$ decays
  - Scale of any NP contributions O(10TeV) or NP has CKM like flavour suppression

- First observation of $B^+ \to \pi^+ \mu\mu$, consistent with SM expectation

- Isospin asymmetry A_I [LHCb-PAPER-2012-011 to be submitted to JHEP]
  - $B \to K^* \mu^+ \mu^-$, A_I results consistent with zero, as expected in SM
  - $B \to K \mu^+ \mu^-$, A_I results sit below the SM expectation in the q^2 region below 4.3 GeV^2/c^4 and above 16 GeV^2/c^4

- A_{CP} in $B^0 \to K^* \gamma$ in good agreement with SM

- LHCb will improve these measurements and has many more measurements in prospect with the 2012 data

Backup

q^2 (GeV^2/c^4) range	Signal Yield	Background Yield
$4m_\mu^2 < q^2 < 2.00$	162.4 ± 14.2	27.7 ± 3.8
$2.00 < q^2 < 4.30$	71.4 ± 10.7	37.1 ± 4.1
$4.30 < q^2 < 8.68$	270.5 ± 18.8	58.8 ± 5.5
$10.09 < q^2 < 12.90$	167.0 ± 14.9	41.7 ± 4.5
$14.18 < q^2 < 16.00$	113.0 ± 11.7	17.1 ± 3.0
$16.00 < q^2 < 19.00$	115.0 ± 12.4	23.9 ± 3.6
$1.00 < q^2 < 6.00$	195.2 ± 16.9	75.8 ± 6.0
$4m_\mu^2 < q^2 < 19.00$	900.0 ± 34.4	206.2 ± 10.3

Table 1: The signal and background yields resulting from a fit to the $K^+\pi^-\mu^+\mu^-$ invariant mass distributions of $B^0 \to K^{*0}\mu^+\mu^-$ candidates in the six q^2-bins used in the analysis, the theoretically 'favoured' $1 < q^2 < 6\,\mathrm{GeV}^2/c^4$ range and in the full q^2-range.

q^2 range (GeV^2/c^4)	dBF/dq^2 ($\times 10^{-7}\,\mathrm{GeV}^{-2}c^4$)	A_{FB}	F_{L}	A_{Im}	$2S_3$
$0.05 < q^2 < 2.00$	$0.68 \pm 0.07 \pm 0.05$	$0.00^{+0.08+0.01}_{-0.07-0.01}$	$0.31^{+0.07+0.03}_{-0.06-0.03}$	$0.06^{+0.11+0.00}_{-0.10-0.03}$	$0.02^{+0.20+0.00}_{-0.21-0.03}$
$2.00 < q^2 < 4.30$	$0.30 \pm 0.05 \pm 0.02$	$-0.20^{+0.08+0.01}_{-0.07-0.03}$	$0.74^{+0.09+0.02}_{-0.08-0.04}$	$-0.02^{+0.10+0.05}_{-0.06-0.01}$	$-0.05^{+0.18+0.05}_{-0.12-0.01}$
$4.30 < q^2 < 8.68$	$0.54 \pm 0.05 \pm 0.05$	$0.16^{+0.05+0.01}_{-0.05-0.01}$	$0.57^{+0.05+0.04}_{-0.05-0.03}$	$0.02^{+0.07+0.01}_{-0.07-0.01}$	$0.18^{+0.13+0.01}_{-0.13-0.01}$
$10.09 < q^2 < 12.89$	$0.50 \pm 0.06 \pm 0.04$	$0.27^{+0.06+0.02}_{-0.06-0.01}$	$0.49^{+0.06+0.03}_{-0.07-0.03}$	$-0.01^{+0.11+0.02}_{-0.11-0.03}$	$-0.22^{+0.20+0.02}_{-0.17-0.03}$
$14.18 < q^2 < 16.00$	$0.59 \pm 0.07 \pm 0.04$	$0.49^{+0.04+0.02}_{-0.06-0.05}$	$0.35^{+0.07+0.07}_{-0.06-0.02}$	$-0.01^{+0.08+0.04}_{-0.07-0.02}$	$0.04^{+0.15+0.04}_{-0.19-0.02}$
$16.00 < q^2 < 19.00$	$0.44 \pm 0.05 \pm 0.03$	$0.30^{+0.07+0.04}_{-0.07-0.01}$	$0.37^{+0.06+0.03}_{-0.07-0.04}$	$0.06^{+0.09+0.03}_{-0.10-0.05}$	$-0.47^{+0.21+0.03}_{-0.10-0.05}$
$1.00 < q^2 < 6.00$	$0.42 \pm 0.04 \pm 0.04$	$-0.18^{+0.06+0.01}_{-0.06-0.02}$	$0.66^{+0.06+0.04}_{-0.06-0.03}$	$0.07^{+0.07+0.02}_{-0.07-0.01}$	$0.10^{+0.15+0.02}_{-0.16-0.01}$

Table 2: Central values for, and statistical and systematic uncertainties on, the differential branching fraction, A_{FB}, F_{L}, A_{Im} and S_3 in bins of q^2. The first uncertainty is statistical and the second systematic.

Background	Background Level (%)	Signal Loss (%)
$B^0 \to K^{*0}\mu^+\mu^-$ (with $K \leftrightarrow \pi$)	0.85 ± 0.02	0.11
$B^0 \to K^{*0}J/\psi$ (with $\pi \leftrightarrow \mu$)	0.27 ± 0.08	0.05
$B^0 \to K^{*0}J/\psi$ (with $K \leftrightarrow \mu$)	0.00 ± 0.00	0.03
$B_s^0 \to \phi\mu^+\mu^-$	1.23 ± 0.50	0.32
$B^+ \to K^+\mu^+\mu^-$	0.14 ± 0.03	–
Total	2.49 ± 0.51	0.52

Theoretical control of form factors

- Recent paper uses experimental results to make a fit to the form factor ratios V/A_1 and A_1/A_2 - green bands show the 1 and 2σ contours
- Blue band shows form factor ratio extracted from light cone sum rules
- Red and orange points show ratio extracted from lattice calculations

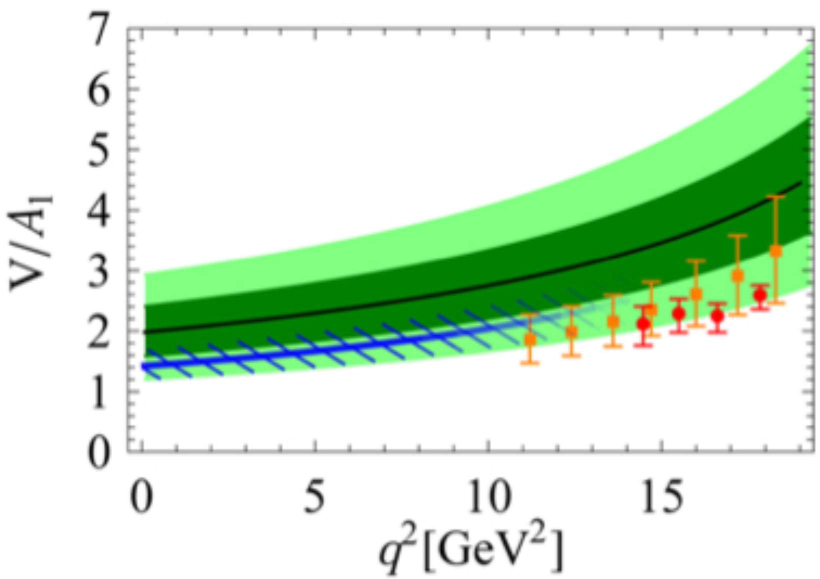

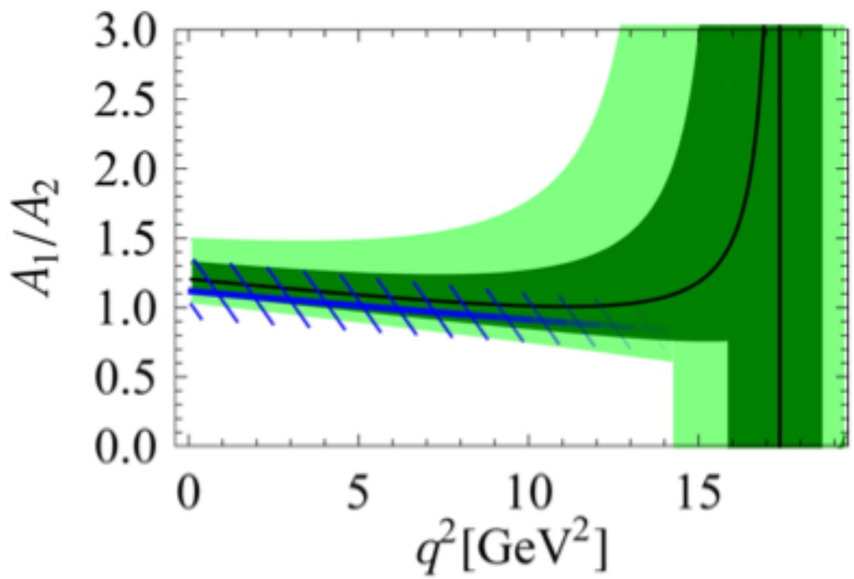

[C. Hambrock and G. Hiller arXiv:1204.4444]

The interest in A_T^2

- C_7 and C_7' are constrained by $b \to s\gamma$ processes. Even in the SM-like allowed region can still have large sensitivity to C_7' through A_T^2
- S_3 is related to A_T^2 through $S_3 = 1/2(1-F_L)A_T^2$

[S. Descotes-Genon et. al., arXiv:1104.3342]

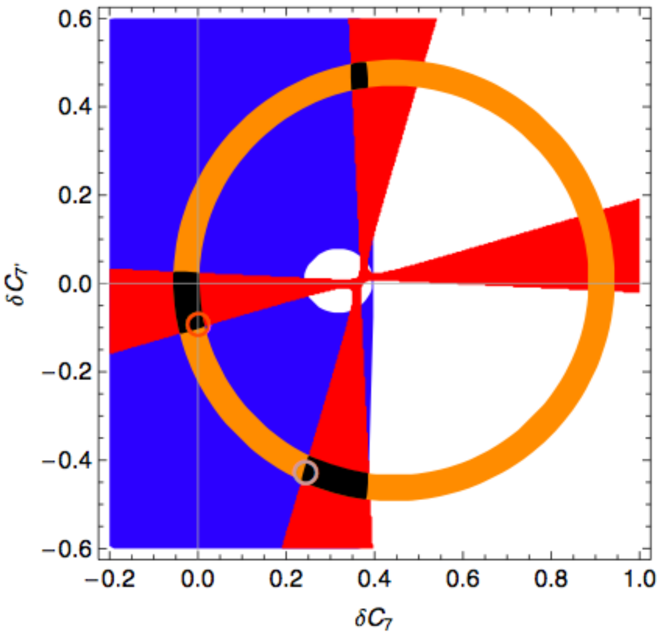

$A_I(K^{*0}\gamma)$, $S_{K^{*0}\gamma}$, $\mathcal{B}(b \to s\gamma)$

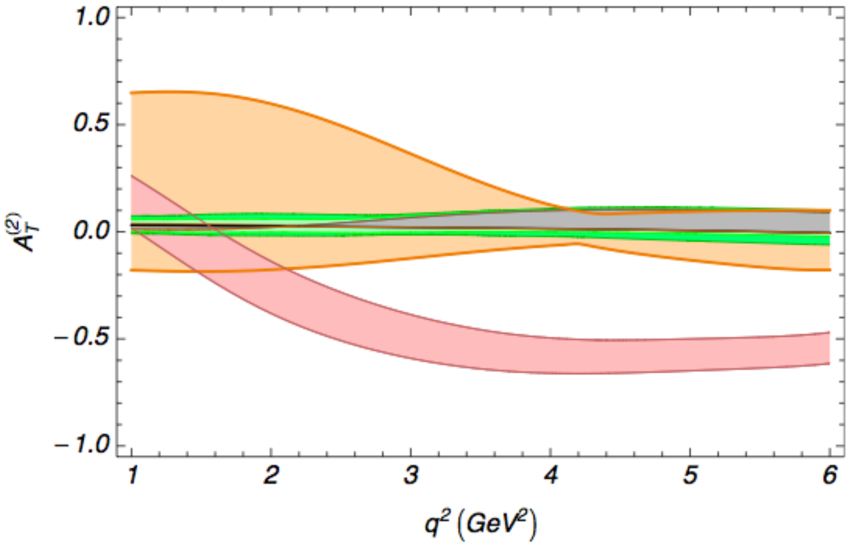

Non-SM like region

SM-like region

Muon Triggers

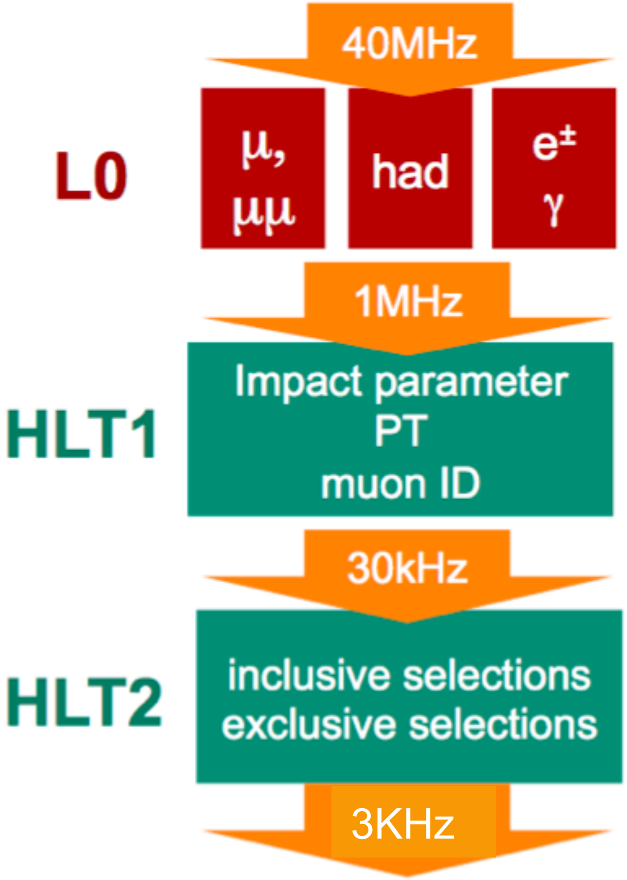

L0 Hardware	Single-μ: p_T> 1.5 GeV/c Di – μ : 2 clean muons p_T1>0.56GeV/c p_T2>0.48GeV/c
HLT1 Software	Single-μ: p_T> 0.8GeV/c IP > 0.11mm, IPS > 5 Single-μ: p_T>1.8GeV/c (no IP)
HLT2 Software	Dimuon: $M_{\mu\mu}$ > 4.7GeV/c^2 Several MVA lines with p_T and vertex displacement cuts

+ Global Event Cuts for events with high multiplicity

- ~1 kHz given to the muon lines
- p_T cuts on muon lines kept very low → trigger efficiency very high

Acceptance Correction

- Correct angular and q^2 distributions for the effect of the detector and selection
  - μ p>3GeV/c → effect on θ_l
  - IP forward-going hadrons → effect on θ_K

- Use a binned acceptance correction derived from LHCb simulation

- Simulation quality verified with range of control channels ($B0 \to K^* J/\psi$, $J/\psi \to \mu\mu$, $D^* \to D^0(K\pi)\pi$)
  - Tracking efficiency
  - Hadron (mis-)identification probabilities
  - Muon (mis-)identification
  - Overall momentum and η distributions

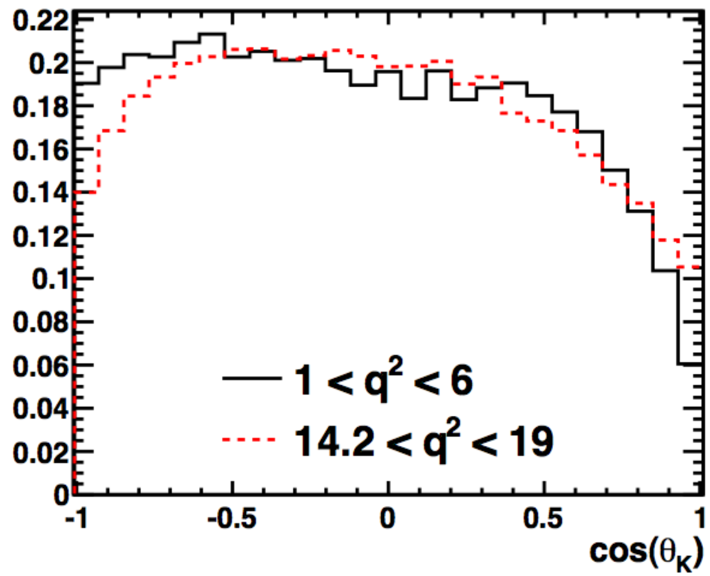

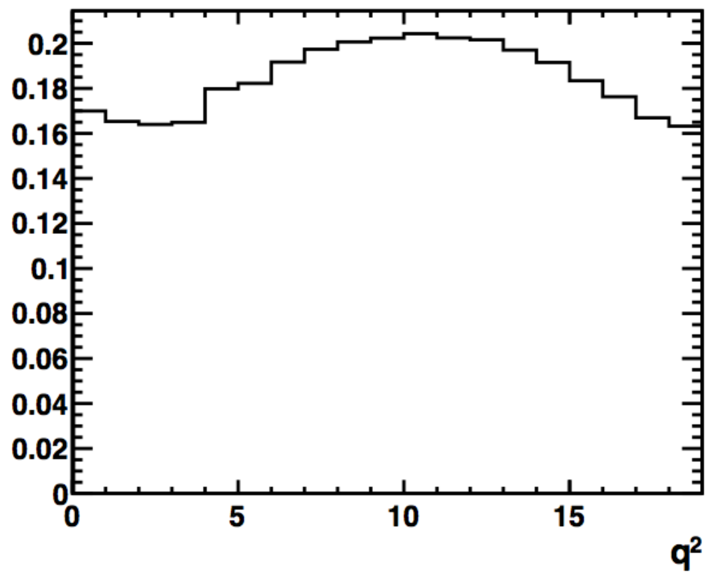

$B \to K^* \ell^+ \ell^-$: low vs. high q^2

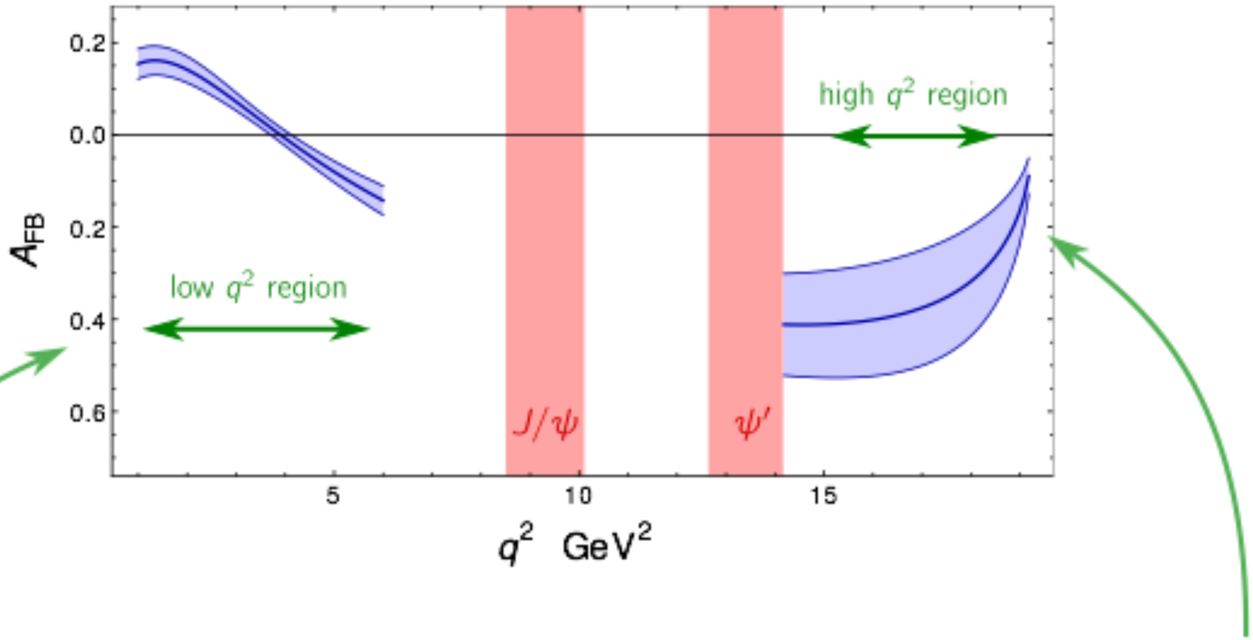

- QCDF: non-factorizable corrections to $O(\alpha_s)$
- LCSR: form factors with correlated uncertainties to all orders in Λ/m_b

[Beneke et al. (2001, 2004); Ball, Zwicky (2004); Altmannshofer et al. (2008); Khodjamirian et al. (2010)]

- OPE in powers of $\Lambda_{QCD}/\sqrt{q^2}$
- Non-perturbative corrections beyond form factors negligible
- form factors poorly known

[Grinstein, Pirjol (2004); Bharucha et al. (2008); Bobeth et al. (2010); Beylich et al. (2011)]

Operators (1)

- Operators
  - Current-current operators [(V-A)]

$$Q_1 = (\bar{b}_\alpha \gamma_\mu P_L q_\beta)(\overline{q}'_\beta \gamma^\mu P_L q''_\alpha),$$
$$Q_2 = (\bar{b} \gamma_\mu P_L q)(\overline{q}' \gamma^\mu P_L q'').$$

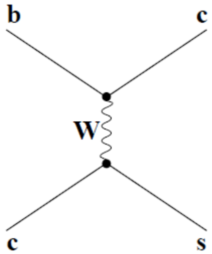

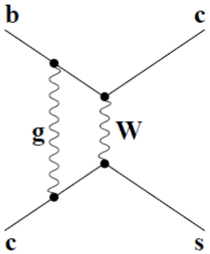

  - Gluonic penguin operators [(V-A) and (V+A)]

$$Q_3 = (\bar{b} \gamma_\mu P_L q) \sum_{q'} (\overline{q}' \gamma^\mu P_L q'),$$
$$Q_4 = (\bar{b}_\alpha \gamma_\mu P_L q_\beta) \sum_{q'} (\overline{q}'_\beta \gamma^\mu P_L q'_\alpha),$$
$$Q_5 = (\bar{b} \gamma_\mu P_L q) \sum_{q'} (\overline{q}' \gamma^\mu P_R q'),$$
$$Q_6 = (\bar{b}_\alpha \gamma_\mu P_L q_\beta) \sum_{q'} (\overline{q}'_\beta \gamma^\mu P_R q'_\alpha);$$

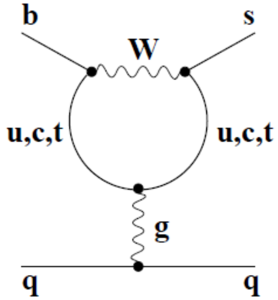

Operators (2)

- Operators
  - Current-current operators [(V-A)]

$$
\begin{aligned}
Q_1 &= (\bar{b}_\alpha \gamma_\mu P_L q_\beta)(\overline{q}'_\beta \gamma^\mu P_L q''_\alpha), \\
Q_2 &= (\bar{b} \gamma_\mu P_L q)(\overline{q}' \gamma^\mu P_L q'').
\end{aligned}
$$

$$
\begin{aligned}
Q_2(\bar{b}\to\bar{c}c\bar{s}) &= (\bar{b}\gamma_\mu P_L c)(c\gamma^\mu P_L \bar{s}), \\
Q_2(\bar{b}\to\bar{c}c\bar{d}) &= (\bar{b}\gamma_\mu P_L c)(c\gamma^\mu P_L \bar{d}), \\
Q_2(\bar{b}\to\bar{c}u\bar{s}) &= (\bar{b}\gamma_\mu P_L c)(u\gamma^\mu P_L \bar{s}), \\
Q_2(\bar{b}\to\bar{c}u\bar{d}) &= (\bar{b}\gamma_\mu P_L c)(u\gamma^\mu P_L \bar{d}), \\
Q_2(\bar{b}\to\bar{u}c\bar{s}) &= (\bar{b}\gamma_\mu P_L u)(c\gamma^\mu P_L \bar{s}), \\
Q_2(\bar{b}\to\bar{u}c\bar{d}) &= (\bar{b}\gamma_\mu P_L u)(c\gamma^\mu P_L \bar{d}), \\
Q_2(\bar{b}\to\bar{u}u\bar{s}) &= (\bar{b}\gamma_\mu P_L u)(u\gamma^\mu P_L \bar{s}), \\
Q_2(\bar{b}\to\bar{u}u\bar{d}) &= (\bar{b}\gamma_\mu P_L u)(u\gamma^\mu P_L \bar{d}).
\end{aligned}
$$

  - Gluonic penguin operators [(V-A) and (V+A)]

$$
\begin{aligned}
Q_3 &= (\bar{b}\gamma_\mu P_L q)\sum_{q'}(\overline{q}'\gamma^\mu P_L q'), \\
Q_4 &= (\bar{b}_\alpha\gamma_\mu P_L q_\beta)\sum_{q'}(\overline{q}'_\beta\gamma^\mu P_L q'_\alpha), \\
Q_5 &= (\bar{b}\gamma_\mu P_L q)\sum_{q'}(\overline{q}'\gamma^\mu P_R q'), \\
Q_6 &= (\bar{b}_\alpha\gamma_\mu P_L q_\beta)\sum_{q'}(\overline{q}'_\beta\gamma^\mu P_R q'_\alpha);
\end{aligned}
$$

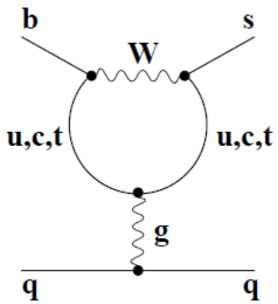

Operators (3)

– Electroweak penguin operators

$$Q_7 = \frac{3}{2}(\bar{b}\gamma_\mu P_L q)\sum_{q'} e_{q'}(\bar{q}'\gamma^\mu P_R q'),$$

$$Q_8 = \frac{3}{2}(\bar{b}_\alpha\gamma_\mu P_L q_\beta)\sum_{q'} e_{q'}(\bar{q}'_\beta\gamma^\mu P_R q'_\alpha),$$

$$Q_9 = \frac{3}{2}(\bar{b}\gamma_\mu P_L q)\sum_{q'} e_{q'}(\bar{q}'\gamma^\mu P_L q'),$$

$$Q_{10} = \frac{3}{2}(\bar{b}_\alpha\gamma_\mu P_L q_\beta)\sum_{q'} e_{q'}(\bar{q}'_\beta\gamma^\mu P_L q'_\alpha);$$

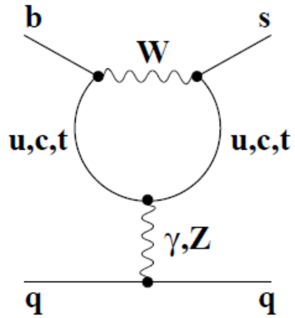

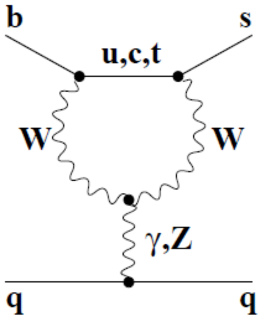

– Magnetic penguin operators

$$Q_{7\gamma} = \frac{e}{8\pi^2} m_b \left[\bar{b}\sigma^{\mu\nu}(1+\gamma_5)q\right] F_{\mu\nu},$$

$$Q_{8g} = \frac{g_s}{16\pi^2} m_b \left[\bar{b}_\alpha\sigma^{\mu\nu}(1+\gamma_5)T_a^{\alpha\beta} q_\beta\right] G^a_{\mu\nu};$$

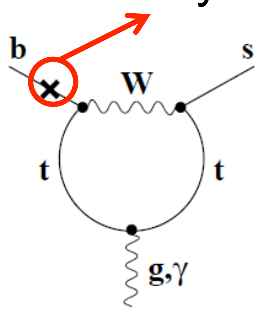

Operators (4)

– Semi-leptonic penguin operators

$$\begin{aligned} Q_{9V} &= (\bar{b}\gamma_\mu P_L q)(\bar{\ell}\gamma^\mu \ell), \\ Q_{10A} &= (\bar{b}\gamma_\mu P_L q)(\bar{\ell}\gamma^\mu \gamma_5 \ell), \\ Q_S &= (\bar{b}\gamma_\mu P_R q)(\bar{\ell}\ell), \\ Q_P &= (\bar{b}\gamma_\mu P_R q)(\bar{\ell}\gamma_5 \ell), \end{aligned}$$

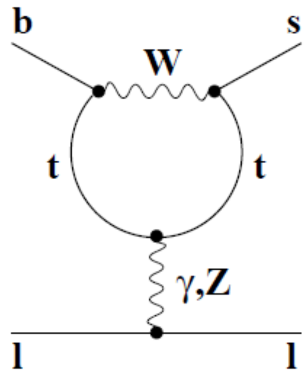

– Here,
  - Q_{9V} represents cases with leptons in a vector final state
  - Q_{10A} represents cases with leptons in an axial final state

– $Q_{S,P}$ only relevant for B→ll decays

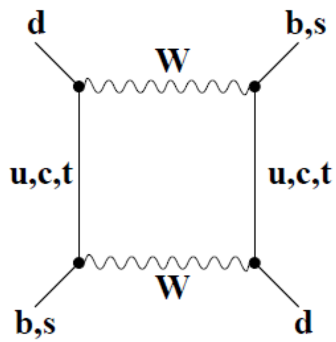

– Note haven't drawn out the box diagram

– Throughout, (with NP) operators could be replaced with a right-handed version Q' where instead of P_L, have P_R